Cell Reports
Physical Science

CellPress
OPEN ACCESS

Article

Deconstruction of unsaturated polymers through photo-mediated oxidation under O_2

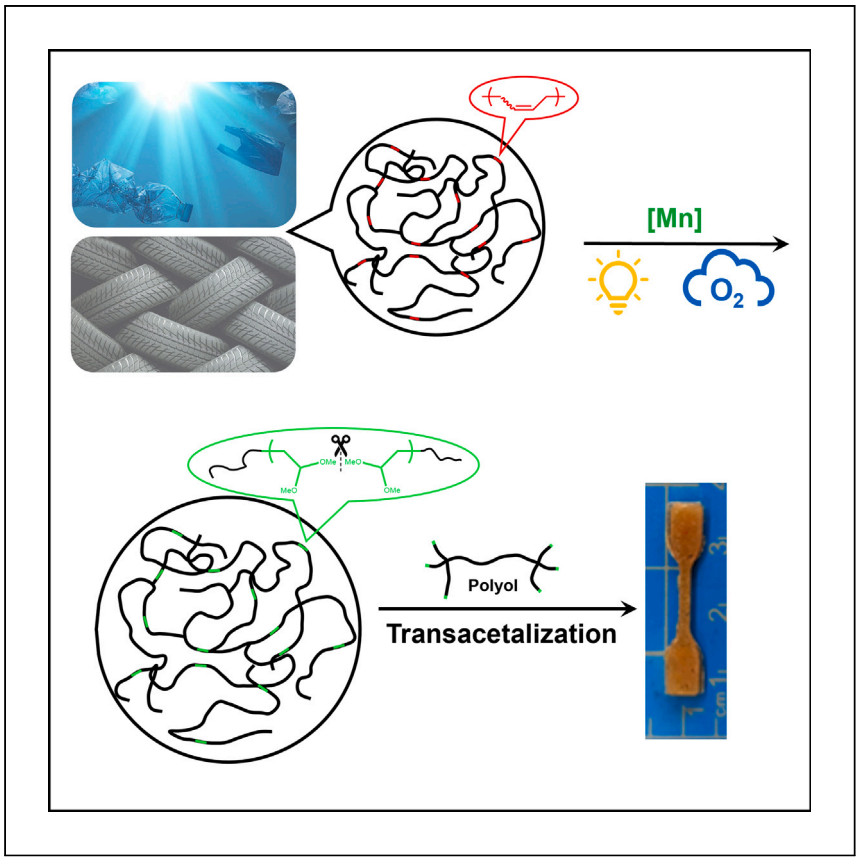

Chen et al. demonstrate the oxidative degradation of unsaturated polymers using O_2 as the oxidant in the presence of an earth-abundant Mn catalyst, under 365 nm light, at ambient temperature and pressure. The process generates acetal functionalized oligomers, which can undergo transacetalization to form polymer networks for reuse of materials.

Hanlin Chen, Xin Guan, Puyan Zhang, Devavrat Sathe, Junpeng Wang

jwang6@uakron.edu

Highlights

Oxidative cleavage of unsaturated polymers proceeds under mild conditions

The use of atmospheric O_2 and Mn catalyst is economical

The degradation products can be reused to make useful materials

Chen et al., Cell Reports Physical Science 5, 102104
August 21, 2024
https://doi.org/10.1016/j.xcrp.2024.102104

Please cite this article in press as: Chen et al., Deconstruction of unsaturated polymers through photo-mediated oxidation under O_2, Cell Reports Physical Science (2024), https://doi.org/10.1016/j.xcrp.2024.102104

Cell Reports
Physical Science

Article

Deconstruction of unsaturated polymers through photo-mediated oxidation under O_2

Hanlin Chen,[1,2] Xin Guan,[1,2] Puyan Zhang,[1] Devavrat Sathe,[1] and Junpeng Wang[1,3,4,*]

SUMMARY

While oxidative cleavage has been a well-known strategy to degrade unsaturated polymers, most processes require harsh conditions and/or expensive oxidizing agents. Using O_2 to degrade polymers is highly desirable, but no reported process is well controlled for the chemical recycling of polymers. Here, we report a photo-mediated oxidative degradation process for unsaturated polymers under O_2 using an earth-abundant Mn catalyst, and the process is demonstrated with polybutadiene, polydicyclopentadiene, and dehydrogenated polyethylene. Nonactivated internal alkenes in these polymers can be effectively cleaved without elevated temperature or pressure. The oxidation process generates acetal as the main functionality, which can be used for further recycling. As a proof of concept, the oligomers with acetal end groups, resulting from the oxidation of polybutadiene, are shown to undergo transacetalization with polyols to form a polymer network. The oxidation process demonstrated here holds promise for the recycling of hydrocarbon polymers under mild conditions in a cost-effective fashion.

INTRODUCTION

Since plastics started to be mass produced in the 1950s, 8.3 billion metric tons of polymers have been produced globally. Most of these polymers were discarded or incinerated, accumulating in land and oceans, and contaminating our environment; only 600 million metric tons of them have been properly recycled.[1] Most commercial polymers, such as polyolefins, which account for over half of the global polymer production, comprise hydrocarbon backbone. The hydrocarbon backbone brings about excellent stability and durability, but it also leads to challenges in recycling.[2] Introducing unsaturation can substantially enhance the reactivity and therefore alleviate the challenges in their recycling.[3–5] In fact, the degradation of unsaturated polymers has been studied for decades, and common methods include pyrolysis,[6] olefin metathesis,[7] and oxidative cleavage.[8]

Conventional methods for oxidative cleavage of alkenes such as those involving ozonolysis,[8] epoxidation,[9] and permanganate oxidation[10] can effectively degrade unsaturated polymers into oligomers and small molecules. These oxidation methods are relatively well controlled and can generate products that are useful for recycling or upcycling.[11–14] However, these approaches typically require conditions that are unfriendly to the environment, costly in energy, and challenging to scale up. For example, ozone is highly corrosive and requires intensive energy to generate and use.[15,16] Moreover, oxidative cleavage involving epoxidation requires additional steps such as hydrolysis and further oxidation.[17] Furthermore, oxidation using $KMnO_4$ requires multiple equivalents of oxidants that generate unwanted by-products during oxidation, causing undesirable secondary contamination.[18]

[1]School of Polymer Science and Polymer Engineering, University of Akron, 170 University Avenue, Akron, OH 44325, USA

[2]These authors contributed equally

[3]X (formerly Twitter): @JPChem1

[4]Lead contact

*Correspondence: jwang6@uakron.edu

https://doi.org/10.1016/j.xcrp.2024.102104

Please cite this article in press as: Chen et al., Deconstruction of unsaturated polymers through photo-mediated oxidation under O_2, Cell Reports Physical Science (2024), https://doi.org/10.1016/j.xcrp.2024.102104

The most ideal oxidant would be O_2, which is abundant, green, and readily accessible. Oxidation by O_2 happens all the time in polymers, which compromises their properties. For example, chemical defects in polyethylene induce the formation of radicals on polyethylene, which can react with O_2 and lead to degradation.[15] In addition, unsaturated polymers can generate stable allylic radicals to react with O_2, generating peroxides, ketones, and alcohols and causing further degradation of polymers.[15,19–22] While these oxidation processes occur in polymers, they are slow for polymer recycling purposes. Adding prodegradants can facilitate oxidative degradation, but these processes are not controlled to generate applicable products for further recycling.[23,24] A catalytic mechanism that promotes the oxidative cleavage of unsaturated polymers under O_2 is highly desirable for the recycling of polymers. To this end, there have been reports on the use of oxygenase enzymes,[25] but to the best of our knowledge, oxidative cleavage of unsaturated polymers with O_2 using a synthetic catalyst has not been reported. The scarcity of efficient catalytic oxidative degradation methods for unsaturated polymers with O_2 may be due to the limited number of catalysts that can activate both the internal nonactivated alkenes[26] and O_2.[27]

A recent study by Xiao and coworkers showed the catalytic oxidation of alkenes with O_2 using a non-heme manganese catalyst $Mn(dtbpy)_2(OTf)_2$ (dtbpy = 4,4-di-*tert*-butyl-2,2′-dipyridyl) (Figure 1A) under visible-light irradiation.[28] Irradiation on the Mn catalyst reduces its redox potential, and the more reducing Mn complex activates O_2, forming an Mn-oxo species that oxidatively cleaves alkenes. Notably, the photo-mediated oxidative cleavage was successfully demonstrated with internal alkenes, such as the C=C bond in cyclooctene, generating functionalities, including aldehyde, ester, acetal, and epoxide.[28] Inspired by this work, we envision that such photo-mediated catalytic oxidation can be applied to the degradation and recycling of unsaturated polymers. Here, we demonstrate the photo-mediated oxidative degradation of unsaturated polymers with O_2 using the non-heme Mn catalyst at room temperature. The resulting oligomers with acetal end groups can be used to form a dynamic polymer network through transacetalization with a polyol. The substrate scope for the photo-mediated catalytic oxidation is extended to crosslinked polymers and dehydrogenated polyolefins.

RESULTS AND DISCUSSION

Photo-mediated oxidative cleavage of non-activated internal alkenes

Following the procedure reported by Xiao and coworkers, we synthesized $Mn(dtbpy)_2(OTf)_2$ and confirmed its structure by X-ray crystallography (Figure S1; Table S1).[28] Note that Xiao and coworkers used 470 nm blue light-emitting diode, which was not available in our lab.[28] For the ease of access, we tested the feasibility of using a sunlamp and a 365-nm photoreactor as alternative irradiation sources (Figure S2) on 1,1-diphenylethylene (DPE). While irradiation with a sunlamp for 16 h showed only 6% conversion, irradiation with 365-nm light for the same duration of time resulted in 50% conversion of DPE (Figure S3; Table S2). The color of the reaction mixture turned from pale yellow to greenish brown after irradiation under the 365-nm light for 5 min. This change in color was also observed by Xiao and colleagues when the irradiation was conducted with 470 nm light and was attributed to the formation of a bis-μ-O_2-Mn_2 complex.[28] The successful oxidation of DPE using the 365-nm light validates its use as the irradiation source for the photo-mediated oxidative cleavage of alkenes.

Since our goal is to apply the photo-mediated oxidation to unsaturated polymers with nonactivated internal alkenes, a model compound that contains this type of

Please cite this article in press as: Chen et al., Deconstruction of unsaturated polymers through photo-mediated oxidation under O_2, Cell Reports Physical Science (2024), https://doi.org/10.1016/j.xcrp.2024.102104

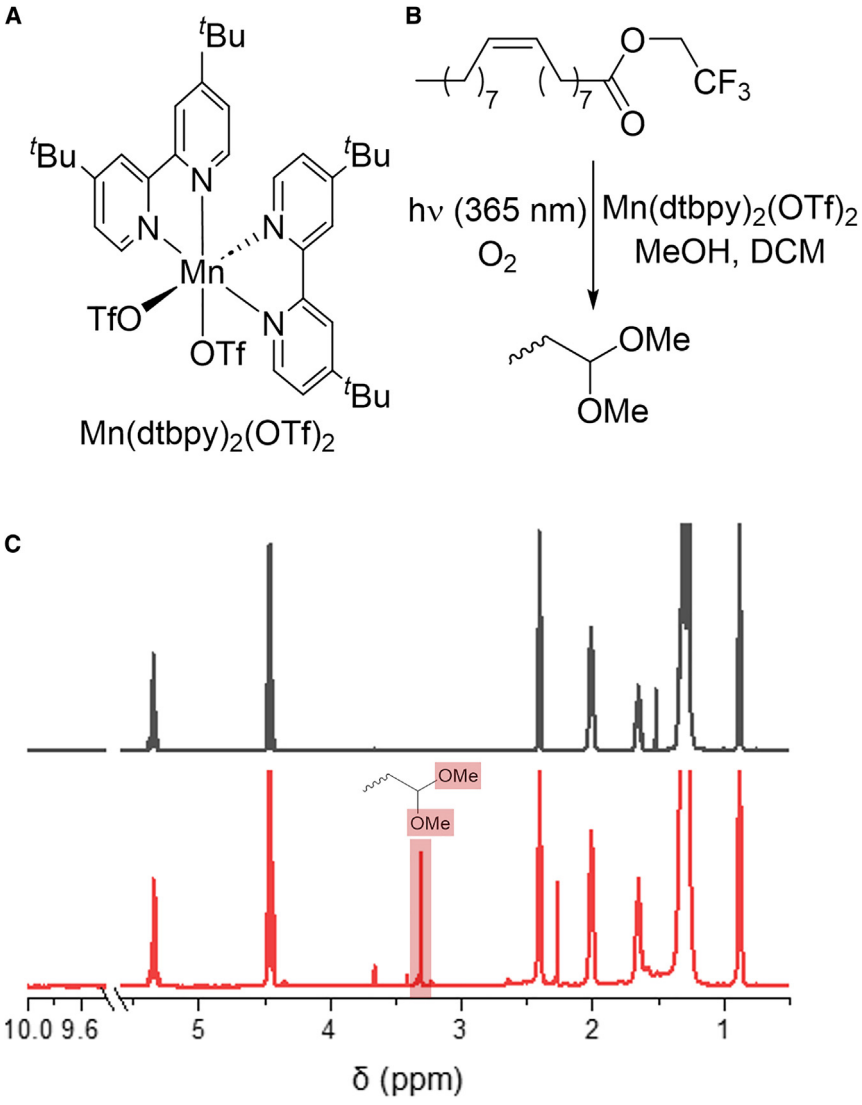

Figure 1. Photo-mediated oxidative cleavage of non-activated internal alkenes catalyzed by a Mn catalyst

(A) The chemical structure of $Mn(dtbpy)_2(OTf)_2$ catalyst.

(B) Reaction scheme for photo-mediated oxidative cleavage of a substrate with non-activated internal alkene TFO.

(C) ^{1}H-NMR before (black) and after (red) the reaction shown in (B) proceeded for 16 h.

See also Figure S4.

alkene is needed to test the reaction and to optimize the reaction condition. For this reason, a nonvolatile unsaturated ester, 2,2,2-trifluoroethyl oleate (TFO; Figure 1B) was selected as the model compound. On the ^{1}H-NMR of TFO, the α-methylene shows a chemical shift of 4.46, which remains unchanged during oxidation and does not overlap with the peaks of oxidation products, such as aldehyde (δ = 9.8 ppm), methyl ester (δ = 3.7 ppm), acetal (δ = 3.3 ppm), and epoxide (δ = 2.9 ppm) (Figure 1C), making it convenient to quantify the conversion and yield.

Optimization of reaction conditions

In previous work conducted on small-molecule substrates, methanol was found to be critical for the success of the oxidative cleavage, and using other solvents alone

Please cite this article in press as: Chen et al., Deconstruction of unsaturated polymers through photo-mediated oxidation under O_2, Cell Reports Physical Science (2024), https://doi.org/10.1016/j.xcrp.2024.102104

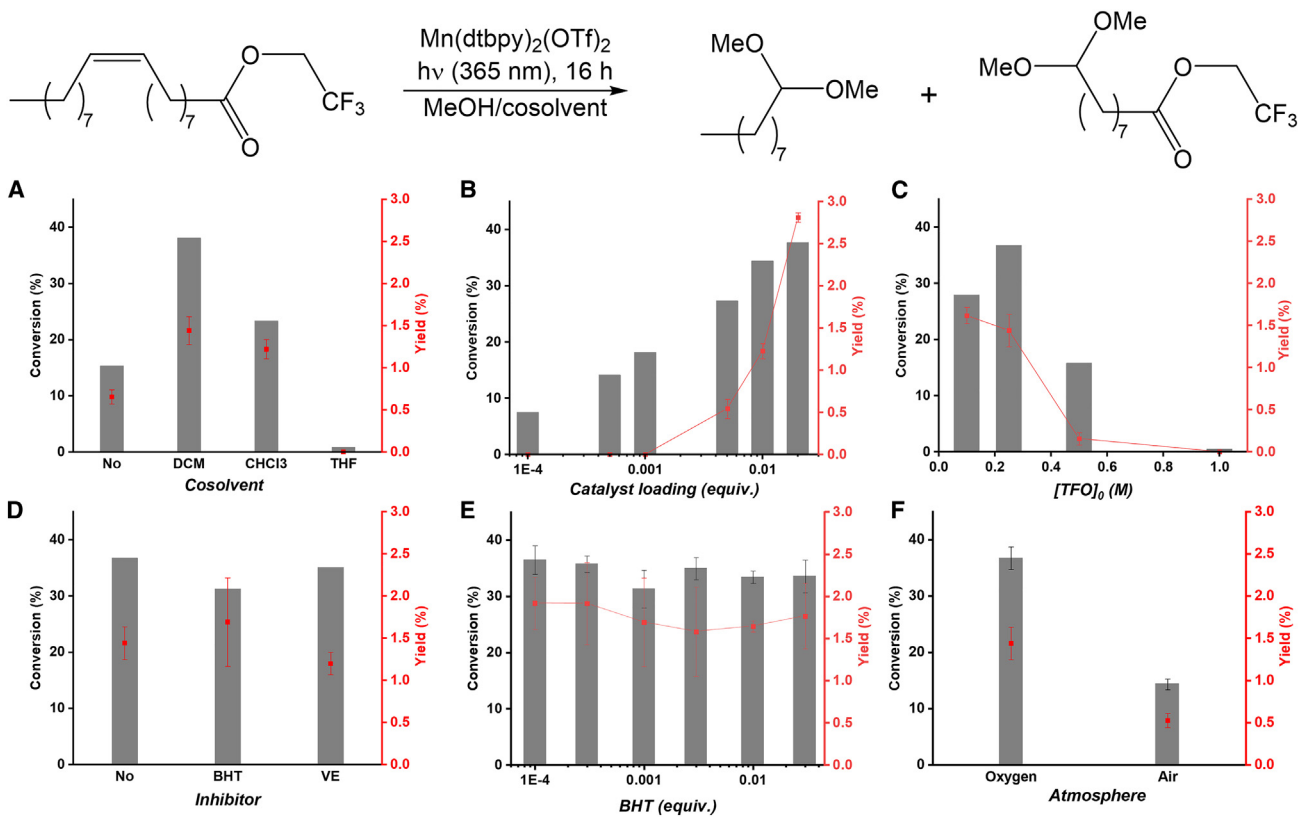

Figure 2. Optimization of the reaction conditions using TFO as the substrate

Conversions are shown as gray columns, and yields of acetal are shown as red squares.

(A) Solvent effect. MeOH was mixed with various cosolvents in a 1:9 v/v ratio, and the reaction was performed under the following conditions: 1 mol % $Mn(dtbpy)_2(OTf)_2$, $[TFO]_0$ = 0.25 M, 1 atm O_2, 365 nm irradiation at room temperature; see also Table S3.

(B) Effect of $Mn(dtbpy)_2(Otf)_2$ catalyst loading ($[TFO]_0$ = 0.25 M, MeOH/DCM [1:9], 1 atm O_2, 365 nm irradiation at room temperature); see also Table S4.

(C) Effect of the initial concentration of the substrate (1 mol % $Mn(dtbpy)_2(OTf)_2$, MeOH/DCM [1:9], 1 atm O_2, 365 nm irradiation at room temperature); see also Table S5.

(D) Effect of inhibitors (1 mol % $Mn(dtbpy)_2(OTf)_2$, 1 mol % inhibitor, $[TFO]_0$ = 0.25 M, MeOH/DCM [1:9], 1 atm O_2, 365 nm irradiation at room temperature); see also Table S6.

(E) Effect of BHT loading (1 mol % $Mn(dtbpy)_2(OTf)_2$, $[TFO]_0$ = 0.25 M, MeOH/DCM [1:9], 1 atm O_2, 365 nm irradiation at room temperature); see also Table S7.

(F) Effect of the atmosphere (1 mol % $Mn(dtbpy)_2(OTf)_2$, $[TFO]_0$ = 0.25 M, MeOH/DCM [1:9], 1 atm O_2 or air, 365 nm irradiation at room temperature); see also Table S8.

In each case, the error bar is the SD of 3 replicates of measurements.

exclusively led to no conversion.[28] It was suggested that methanol facilitates the activation of the Mn complex $Mn(dtbpy)_2(OTf)_2$. Since we aim to apply the oxidative degradation to polymers, a suitable solvent system that is a good solvent for typical unsaturated polymers is needed; while methanol gave the optimal oxidation, it is a poor solvent for common unsaturated polymers, such as polybutadiene (PB). Good solvents for PB, including dichloromethane (DCM), chloroform, and tetrahydrofuran (THF) were mixed with methanol, and TFO was dissolved in the solvent mixture and irradiated under 365-nm light in the presence of 1 atm O_2 and $Mn(dtbpy)_2(OTf)_2$ for 16 h. It was found that higher conversions of alkene were obtained when using halogenated cosolvent, such as DCM and chloroform (Figure 2A; Table S3). For example, oxidation in a MeOH/DCM (1/9 v/v) mixture showed 38% conversion, while the value was 15% for pure MeOH. The increased conversions obtained when using halogenated cosolvents are favorable for the application of this method to unsaturated polymers, which typically dissolve well in halogenated solvents. For the reaction

Please cite this article in press as: Chen et al., Deconstruction of unsaturated polymers through photo-mediated oxidation under O_2, Cell Reports Physical Science (2024), https://doi.org/10.1016/j.xcrp.2024.102104

done in DCM, acetal (δ = 3.3 ppm) was found to be the most pronounced product in ^{1}H-NMR, and the formation of other functional groups, such as aldehyde (δ 9.8 ppm), ester (δ 3.7 ppm), and epoxide (δ 2.9 ppm), were insignificant (Figures 1C and S4).

The stoichiometry of the catalyst and the concentration of the substrate were also varied to optimize the condition for oxidation. As the catalyst loading increased, both the conversion of alkene and the yield of acetal increased. Since the conversion from 1 mol % catalyst loading (35%) is comparable to the conversion from 2 mol % catalyst loading (38%), 1 mol % catalyst loading was chosen for future optimized experiments. When the catalyst loading was reduced to 0.1 mol %, 18.2% conversion in degradation was still obtained (Figure 2B; Table S4). The optimal concentration of substrate was found to be 0.25 M (Figure 2C; Table S5); higher concentrations led to a reduction in the conversion of alkene and the yield of acetal.

Mechanistic analysis

It was proposed that the mechanism of oxidation involves radical intermediates.[28] To gain insights into the mechanism, radical inhibitors, including butylated hydroxytoluene (BHT) and α-tocopherol were added to the reaction mixture before irradiation. Notably, the two inhibitors did not significantly affect the conversion of alkene or the yield of acetal (Figure 2D; Table S6). Since inhibitors are typically present as stabilizers in commercial unsaturated polymers, the present study indicates that stabilizers in commercial polymers may not need to be removed before applying the photo-mediated oxidation. Further study with the amount of BHT varied showed that the amount of BHT loading (within the range of 0.01–3 mol %) did not significantly affect the conversion of alkene and the yield of acetal (Figure 2E; Table S7). A BHT loading of 0.3 mol % was chosen for future study to account for the presence of stabilizers in commercial polymers.

It is noteworthy that the oxidation does not have to be conducted using pure O_2. Oxidation in an ambient atmosphere also consumed alkene and formed acetal (Figure 2F; Table S8). Although the conversion of alkene and the yield of acetal were lower than those obtained when the reaction was done under pure O_2, the yields calculated based on reacted alkene are comparable, indicating that using air only slowed down the reaction due to a lower concentration of O_2 (Table S8).

While acetal was the most pronounced among the formed functional groups (i.e., acetal, aldehyde, ester, and epoxide), its yield was still much lower than the overall conversion of olefins. The acetal was most likely formed from the acetalization of aldehyde, which was generated from the oxidation of alkene.[28] The low yield of acetal may be due to the photodecomposition of aldehyde that occurs through a radical mechanism under irradiation, generating hydrocarbons.[29,30] In other words, the competition between decomposition and acetalization of acetal was in play. The absence of other significant functionalities on ^{1}H-NMR also supports the formation of hydrocarbons. Irradiation of chlorinated solvents such as DCM and chloroform may generate small amounts of hydrochloric acid,[31,32] which can facilitate the acetalization of aldehyde in MeOH; the promoted yield when DCM or chloroform was used as a cosolvent could be attributed to an enhanced rate in acetalization.

In Xiao and coworkers' study, zeroth-order kinetics in the alkene substrate with respect to time was observed. The reaction showed an induction period, during which an Mn dimer, bis-μ-O_2-Mn_2, was formed. The activation of the Mn dimer, to generate active Mn(IV) species, was proposed to be the rate-determining

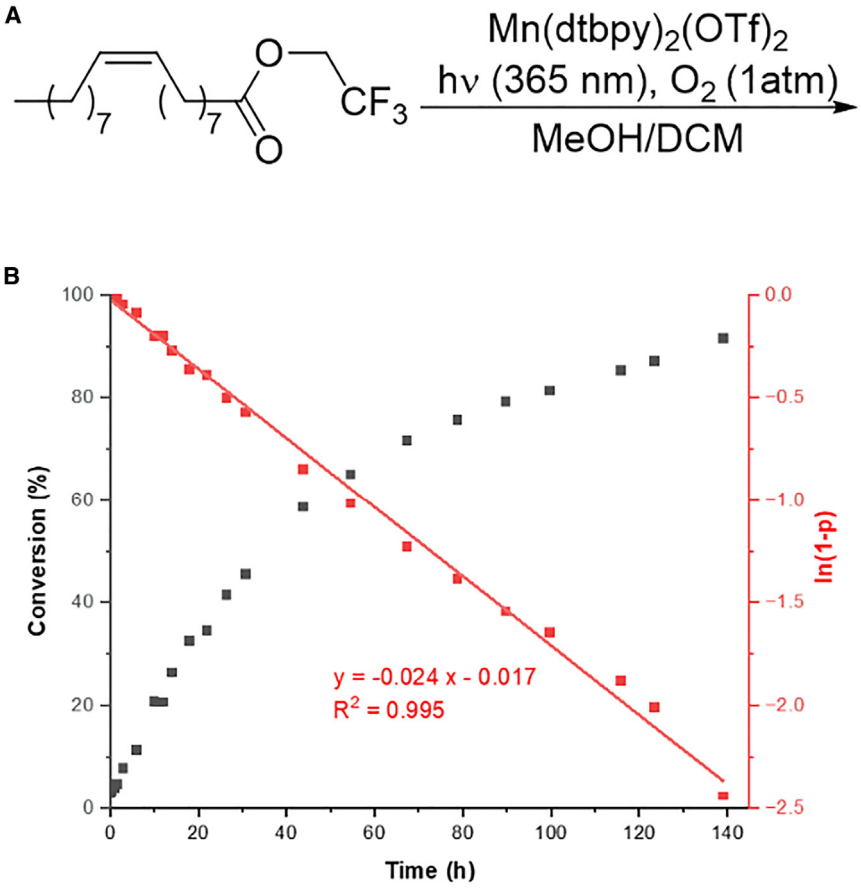

Figure 3. Kinetic study of the photo-mediated oxidation of TFO

(A) Reaction scheme for the photo-mediated oxidation of TFO; reaction condition: 1 mol % $Mn(dtbpy)_2(OTf)_2$, 0.3 mol % BHT, $[TFO]_0$ = 0.25 M, MeOH/DCM (1:9), 1 atm O_2, 365 nm irradiation at room temperature.

(B) Plots of conversion p (in black) and ln(1−p) (in red) against reaction time.

step.[28] Being aware of the differences in light sources and types of alkenes between our work and that of Xiao et al. (365 nm vs. 470 nm and non-activated alkene vs. activated alkene), we performed a kinetic study to probe whether these changes would result in different mechanisms. The reaction was conducted under the optimized conditions (1 mol % $Mn(dtbpy)_2(OTf)_2$, 0.3 mol % BHT, $[TFO]_0$ = 0.25 M, DCM/methanol (v/v 9/1), 1 atm O_2, under 365 nm irradiation at room temperature; Figure 3A) and was monitored using ^{1}H-NMR. As shown in Figure 3B, no induction period was observed at the very beginning of the reaction, which could be due to faster activation of $Mn(dtbpy)_2(OTf)_2$ under 365 nm irradiation. It took ~40 h to reach 50% conversion. At 140 h, the conversion reached over 90%. The conversion increased linearly over time in the first 20 h, but the reaction across the whole time did not obey zeroth-order kinetics; instead, the conversion of the substrate showed a first-order kinetics with respect to time (Figure 3B), indicating that the activation of the non-activated internal alkene is likely involved in the rate-determining step. In addition, an on/off experiment was conducted (Figure S5): the reaction was irradiated for 4 h followed by 2 h of darkness and 6 h of irradiation. It was observed that the rate of the reaction during the dark period was substantially lower than the irradiated period, indicating that irradiation plays an important role in the catalytic cycle.

Cell Reports
Physical Science
Article

CellPress
OPEN ACCESS

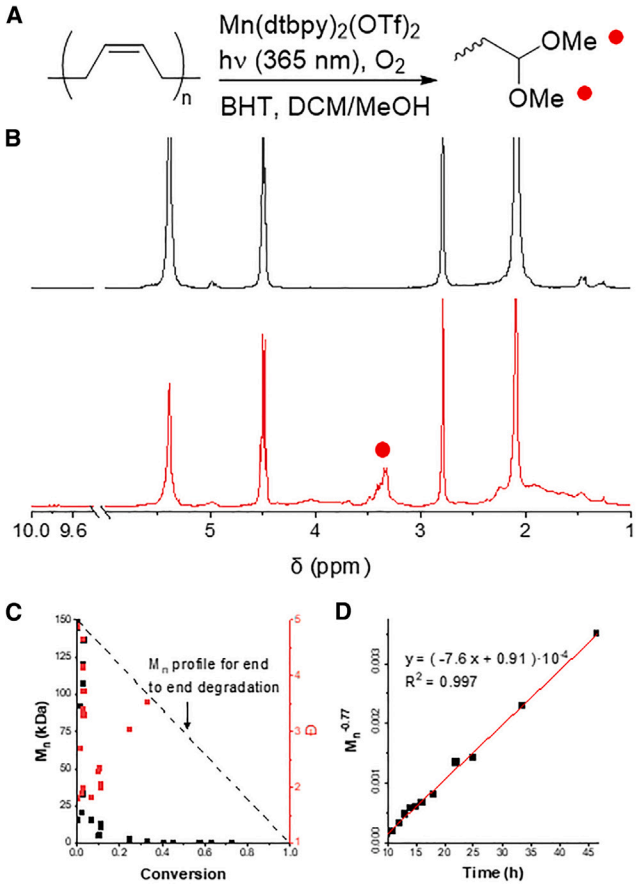

Figure 4. Photo-mediated oxidative degradation of PB (1 g PB, 1 mol % $Mn(dtbpy)_2(OTf)_2$, 0.3 mol % BHT, [olefin] = 0.25 M, DCM/MeOH [9/1], 1 atm O_2, 365 nm irradiation at room temperature)

(A) The oxidation of PB under the optimized condition selectively generates acetal functionality.

(B) ^{1}H-NMR spectra before (black) and after (red) 80 h of photo-mediated degradation.

(C) Plot of M_n against conversion; see also Table S11.

(D) Plot of $M_n^{-0.77}$ against time.

Oxidative degradation of unsaturated polymers

Encouraged by the success with small-molecule non-activated internal alkenes, we demonstrated the oxidative degradation of unsaturated polymers. The conversion for the oxidative degradation of PB was determined by comparing the integration of the olefin peak at 5.40 ppm with that of the internal standard (bis(2,2,2-trifluoroethyl) succinate) at 4.50 ppm (Figures 4B and S9). Various good solvents for PB were mixed with methanol (cosolvent/methanol = 9/1 v/v) for the photo-mediated oxidative degradation (1 mol % $Mn(dtbpy)_2(OTf)_2$, 0.3 mol % BHT, $[alkene]_0$ = 0.25 M, 1 atm O_2, under 365 nm irradiation, at room temperature), and the mixture of MeOH and DCM gave the highest conversions (53% in 16 h; Figure S6). The rate of oxidation was found to be insensitive to the amount of BHT (Table S10; Figure S8). When O_2 was replaced with air while other conditions were kept identical, 13.0% of conversion was obtained (Table S11). In addition to the oxygen concentration, the light intensity also affected the rate of oxidation (Table S9; Figure S7). The occurrence of a significant peak at around 3.3 ppm suggests a selective formation of acetal functional group (Figures 4A, 4B, and S10). The formation of acetal was further supported by Fourier transform infrared (FTIR) characterization, which showed

increased peak intensity in the range of 1,300–1,000 cm^{-1} that corresponds to C–O stretch (Figure S11). The acetal functionality can be used to form a dynamic network with polyol via transacetalization.[33]

A kinetic study showed that the degradation can reach a conversion of over 70% after 5 days of irradiation (Figure 4C). The degradation products were also characterized by gel permeation chromatography (GPC; Figure S12), which showed that the molecular weight of PB was reduced from 150 kDa to <500 Da at ~40% conversion. Further degradation led to molecular weights that cannot be accurately analyzed by GPC. To better understand the mechanism of degradation, The kinetic data were fit to Equation 1,

$$M_{n,t}^{-\alpha} = M_{n,0}^{-\alpha} + \alpha\left(\frac{k}{M_{mon}^{\alpha}}\right)\cdot t \qquad \text{(Equation 1)}$$

in which $M_{n,0}$ and $M_{n,t}$ are the molecular weights of the polymer at the beginning and at time t, respectively, M_{mon} is the molecular weight of the monomer, k is the rate constant of degradation, and α is a factor that describes the dependence of the reactivity on molecular weight. This model was initially proposed by Basedow et al. to understand the hydrolysis of dextran. The model assumes that the rate of bond breaking is proportional to the number of bonds in the polymer raised to the power α.[34] It was also used to analyze the kinetics of other fragmentation processes.[35–37] For a perfect random scission, α = 1, and thus the inverse of molecular weight $1/M_n$ should have a linear relationship with the reaction time. The fitting for our photo-mediated degradation system gave an α of 0.77 (Figure 4D), suggesting that the degradation process is close to random scission.

The selective formation of acetal from oxidative degradation allows the degradation products to be readily reused, since transacetalization chemistry has been applied to supramolecular assembly,[38] therapeutic delivery,[39,40] and vitrimers,[41,42] thanks to its dynamic nature. The transacetalization process involves the exchange of two acetals or the alcoholysis of acetal with a free hydroxy group catalyzed by acid. As a proof of concept, we tested the feasibility of making a polymer network using the degraded products. PB was degraded under the optimized conditions (1 mol % $Mn(dtbpy)_2(OTf)_2$, 0.3 mol % BHT, $[TFO]_0$ = 0.25 M, DCM/methanol (v/v 9/1), 1 atm O_2, under 365 nm irradiation at room temperature), and the resulting solution was directly mixed with 0.4 equiv dipentaerythritol and 0.5 mol % *p*-toluenesulfonic acid (*p*-TSA) and cured in a dog-bone mold at 80°C for 24 h (Figure 5A). The resulting specimen was subjected to tensile test, which gave a Young's modulus of 0.08 ± 0.02 MPa and tensile strength of 0.22 ± 0.01 MPa (Figures 5B and S17). Breakages and relaxations at multiple positions were usually observed before the entire breakage, resulting in a jagged tensile curve. To demonstrate the dynamic nature of the network, a specimen was heated at 80°C in a mixture of ethanol/toluene (1/2 v/v), and after 24 h of heating, it was found that the specimen dissolved completely (Figure S18). In contrast, the specimen did not dissolve when it was heated in pure toluene under otherwise identical conditions, suggesting that transacetalization is required for the dissolution of the specimen. While the mechanical properties of the specimen can be optimized, the formation of a dynamic polymer network using the degradation products highlights the value of the oxidative degradation in recycling and upcycling of unsaturated polymers.

The photo-mediated degradation can be applied to not only linear polymers but also crosslinked ones. Polydicyclopentadiene (PDCPD), which is a high-performance unsaturated thermoset but challenging to recycle,[43] was used as an example to demonstrate the feasibility of degradation. A PDCPD sample was

Cell Reports
Physical Science
Article

CellPress
OPEN ACCESS

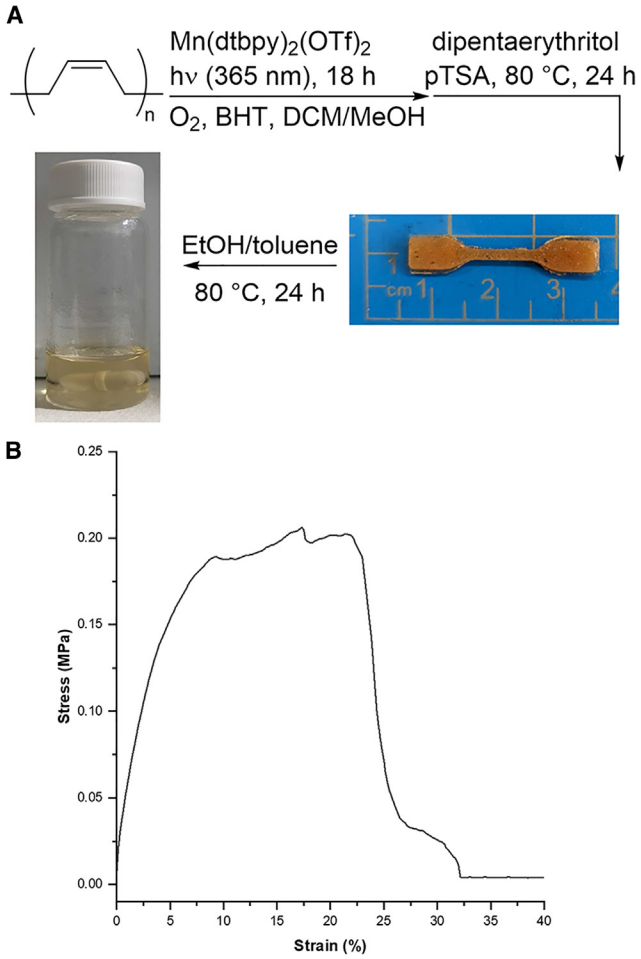

Figure 5. Reuse of the products from the oxidative degradation of PB

(A) A polymer network specimen was made by heating the degradation products of PB with 0.4 equiv dipentaerythritol and 0.5 mol % *p*-TSA at 80°C for 24 h.

(B) A representative tensile testing result for the dynamic polymer network; see also Figure S17.

ground and swollen in a vial, and to the vial was added a $Mn(dtbpy)_2(OTf)_2$ solution in methanol. The mixture was subjected to irradiation for 18 h. The FTIR spectrum of the UV-irradiated PDCPD sample showed an increased peak intensity in the range of 1,300–1,000 cm^{-1}, which supports the formation of acetal (Figure S16). The weight of the solid in the resulting suspension was compared with the initial weight to determine the weight loss. As the cosolvent (in which the PDCPD sample was swollen) was changed, the weight loss correlated well to the swelling ratio of PDCPD in the corresponding methanol/cosolvent mixture (Figure 6). When using the mixture of toluene and MeOH for degradation, almost no change in the weight of the material was observed; when toluene was replaced with chloroform, ~80% weight loss was observed. Based on the degradation kinetics of PB, 18 h of irradiation led to 33% degradation. PDCPD is highly crosslinked, which makes it difficult for the catalyst to penetrate through the network; thus, the conversion of degradation in PDCPD is likely lower than 33%, but it already broke down the polymer network sufficiently so that it dissolved in the sol fraction. This result is consistent with previous work by Johnson and coworkers, in which they found that only a small fraction of bonds on the backbone of PDCPD needs to be cleaved to convert it into a thermoplastic.[43]

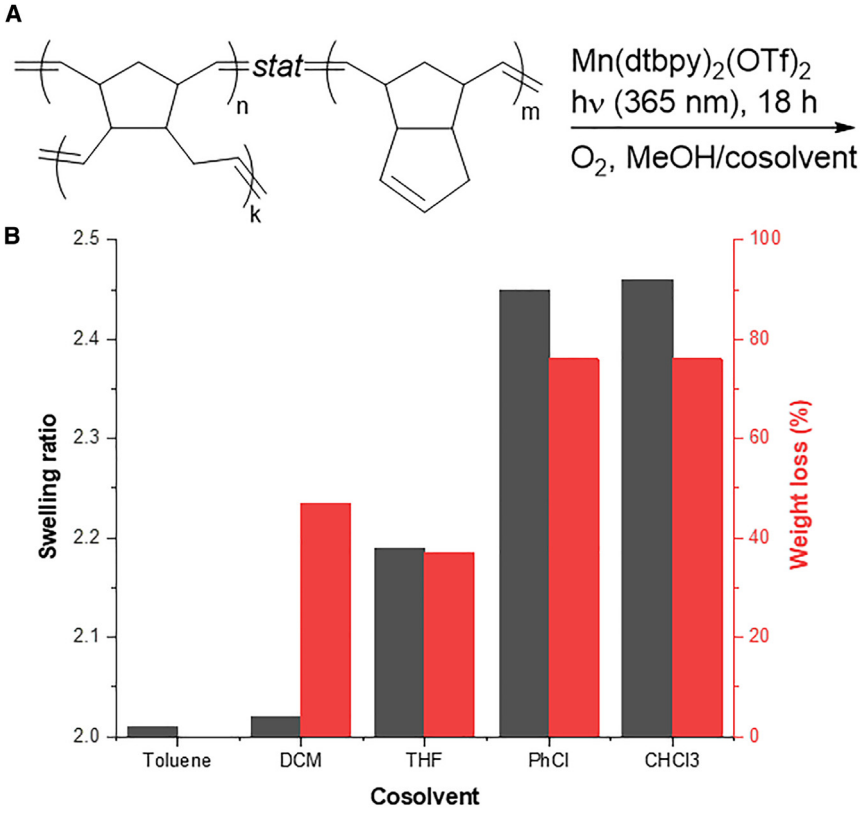

Figure 6. Photo-mediated oxidative degradation of PDCPD in various solvents mixed with methanol

(A) Reaction scheme.

(B) Swelling ratio (black) and weight loss (red) after oxidation as the cosolvent (that was mixed with methanol) was changed for the experiments.

The process of photo-mediated oxidative degradation can also be used to address the recycling of polyolefins. As a preliminary test, high-density polyethylene (HDPE) was subjected to dehydrogenation using an Ir catalyst, which resulted in 2.3% dehydrogenation. The dehydrogenated HDPE (DH-HDPE) was subjected to the following degradation conductions: 1 mol % $Mn(OTf)_2$, 2 mol % dtbpy, 0.3 mol % BHT, 365 nm irradiation in MeOH/PhCl 1:9 v/v, 1 atm O_2, under 365 nm irradiation at room temperature. After 18 h of degradation, the content of olefin dropped to 1.1%, corresponding to a 52% conversion of alkene, in which 36% was converted into acetal (Figure S13). In addition, FTIR spectrum of the UV-irradiated DH-HDPE sample showed an increased peak intensity in the range of 1,300–1,000 cm^{-1}, which is consistent with the formation of acetal (Figure S14). Meanwhile, the molecular weight of DH-HDPE decreased from 31 to 7.3 kDa (Figure S15). These results highlight the feasibility of applying photo-mediated oxidation for the chemical recycling of polyolefins.

In conclusion, we demonstrated the photo-mediated Mn-catalyzed oxidative degradation of unsaturated polymers under O_2. This degradation process complements existing oxidative degradation methods of polymers,[44–46] as it does not require elevated pressure or temperature and can be conducted simply using air. It can reduce the molecular weight of the PB from 150 kDa to <500 Da and selectively generate acetal as the major functional group. The oxidation of internal alkenes shows a first-order kinetics in the alkene substrate with respect to time. The oxidative

Please cite this article in press as: Chen et al., Deconstruction of unsaturated polymers through photo-mediated oxidation under O_2, Cell Reports Physical Science (2024), https://doi.org/10.1016/j.xcrp.2024.102104

degradation was applied to unsaturated polymers, and the degradation mechanism is close to random scission. This method can be applied to address the recycling of both linear and crosslinked polymers. A dynamic polymer network was made from the degradation products of PB, indicating the potential of using this method for upcycling polymers. The oxidative degradation of dehydrogenated polyolefins further highlights its broad scope of use in the chemical recycling of polymers in a sustainable and environmentally friendly fashion.

EXPERIMENTAL PROCEDURES

Resource availability

Lead contact

Further information and requests for resources should be directed to and will be fulfilled by the lead contact, Junpeng Wang (jwang6@uakron.edu).

Materials availability

No unique reagents were generated by this study.

Data and code availability

All data generated by this study are available in the manuscript and supplemental information are available from the lead contact upon request. This paper does not report original code.

Chemicals and materials

The $Mn(dtbpy)_2(OTf)_2$ catalyst used for photo-mediated oxidative degradation and the catalyst Ir-tBuPOCOP catalyst used for dehydrogenation of polyethylene were prepared according to reported procedures.[4,28] PB (98% *cis*-1,4, number average molecular weight [M_n] = 150 kDa), Mn bis(trifluoromethanesulfonate) ($Mn(OTf)_2$), BHT, maleic anhydride, sodium hydride, 2,2,2-trifluoroethanol (TFE), 4-(dimethylamino)pyridine (DMAP), *p*-TSA, dipentaerythritol, and Grubbs second-generation catalyst (G2) were purchased from Sigma-Aldrich. dtbpy, α-tocopherol, di-*tert*-butylchlorophosphine, and borane dimethyl sulfide ($DMS{\cdot}BH_3$) were purchased from TCI. DPE, erucic acid, 5-methoxyresorcinol, and 3,3-dimethyl-1-butene were purchased from Thermo Fisher Scientific. *cis*-2-butene-1,4-diol and oleic acid were purchased from Alfa Aesar. 1-Ethyl-3-(3-dimethylaminopropyl)carbodiimide hydrochloride (EDC) was purchased from Chem-Impex. All solvents were purchased from Thermo Fisher Scientific. All alcohol-type solvents were dried with molecular sieves before use. THF was purified by running through an aluminum oxide plug before use. Other solvents were used directly as received.

NMR characterization

^1H- and ^{13}C-NMR spectra were collected on NMR spectrometers (400 or 500 MHz), and the residual solvent peaks ($CDCl_3$ 7.26 ppm [^1H], 77.16 ppm [^{13}C], 1,1,2,2-tetrachloroethane-d2, 6.0 ppm [^1H]) were used as internal references.

Mechanical testing

Uniaxial tensile testing was performed on an RSA-G2 Solids Analyzer. Grip separation was used as the gauge length for calculating strain. A constant linear rate of 1 mm/mm/min was used as the strain rate. Young's moduli were determined from the slope of the fitted line to the linear 1% deformation region.

A representative procedure of photo-mediated oxidation

A 20-mL vial with a septum was charged with TFO (0.25 mmol, 1.0 equiv) and 890 μL DCM, followed by the addition of BHT (0.165 mg, 0.75 μmol, 0.003 equiv) in 10 μL

DCM and $Mn(dtbpy)_2(OTf)_2$ (2.22 mg, 2.5 μmol, 0.01 equiv) in 100 μL methanol. After purging with oxygen, the vial was connected to an oxygen balloon and subjected to irradiation under 365 nm for 16 h. Volatiles in the resulting mixture were removed under reduced pressure. The mixture was then directly characterized by ^{1}H-NMR to determine the conversion of alkene and yields of functional groups. Protons in the trifluoroethyl group were used as internal standard for calculating conversions and yields.

Procedure for kinetic study of the photo-mediated oxidative degradation of PB

PB (1.0 g, 18.5 mmol, 1 equiv), BHT (12.2 mg, 0.056 mmol, 0.003 equiv), and 66 mL DCM were charged to a round-bottom flask and stirred until fully dissolved, followed by the addition of $Mn(dtbpy)_2(OTf)_2$ (164.5 mg, 0.185 μmol, 0.01 equiv) in 7.3 mL MeOH. After the mixture was stirred in the dark for an additional 30 min to ensure that the polymers were fully dissolved, the flask was equipped with a condenser, connected to an oxygen gas line, and subjected to irradiation. Aliquots taken at various time periods were dried under reduced pressure. GPC was performed after dissolving the mixture in THF. bis(2,2,2-Trifluoroethyl) succinate[47] (1,043.9 mg, 3.700 mmol in $CDCl_3$ stock solution; ^{1}H-NMR (500 MHz, $CDCl_3$): δ 4.49 (q, J = 8.3 Hz, 4H), 2.79 (s, 4H)) was added as an internal standard before ^{1}H-NMR characterizations. The conversion of oxidative degradation was determined by the loss of olefin signal compared to the internal standard after degradation, and the yields are determined by the ratio of integral between the functional groups and internal standards.

Procedure for the photo-mediated oxidative degradation of PDCPD

PDCPD was ground into powder using a Retsch CryoMill. The PDCPD powder (18.5 mg, 0.28 mmol, 1.0 equiv) and 1,120 μL solvent (e.g., toluene, DCM, THF, chlorobenzene, chloroform) were added to a vial. The mixture was allowed to swell overnight. To the vial was added $Mn(dtbpy)_2(OTf)_2$ (5.0 mg, 5.6 μmol, 0.02 equiv) in 1,120 μL MeOH, and the vial was connected to a balloon charged with oxygen and subjected to irradiation for 18 h. The resulting mixture was filtered and washed. The residual solid was dried under vacuum before being collected and weighed to determine weight loss.

Preparation of the polymer network specimens for tensile testing

A vial with 1 g PB was subjected to photo-mediated oxidative degradation for 24 h, and ^{1}H-NMR of the reaction mixture showed that 0.9 mmol acetal was generated. To the mixture were then added dipentaerythritol (49 mg, 0.36 mmol, 0.4 equiv) in 10 mL MeOH and *p*-TSA (0.78 mg, 0.005 mmol, 0.005 equiv) in 100 μL MeOH. Solvents were removed under reduced pressure, resulting in orange syrup. The mixture was added into a Teflon mold (ASTM D638 type IV in 25% scale) and degassed under vacuum for 2 h. The mixture was then warmed up to 80°C, heated at 80°C for 10 min, and connected to vacuum for additional degassing. The mixture was cured at 80°C for 24 h to render the specimens for tensile tests.

Synthesis of TFO

Oleic acid (5.7 g, 20 mmol, 1.0 equiv), TFE (2.4 g, 24 mmol, 1.2 equiv), EDC (7.7 g, 40 mmol, 2.0 equiv), DMAP (586 mg, 4.8 mmol, 0.24 equiv), and 70 mL DCM were charged to a round-bottom flask and stirred under nitrogen overnight. After the removal of volatiles using a rotary evaporator, the mixture was purified by column chromatography using ethyl acetate and hexane, resulting in a colorless liquid. ^{1}H-NMR (500 MHz, $CDCl_3$, ppm): δ 5.44–5.23 (m, 2H), 4.46 (q, J = 8.5 Hz, 2H),

2.41 (t, J = 7.5 Hz, 2H), 2.10–1.93 (m, 4H), 1.66 (p, J = 7.5 Hz, 2H), 1.45–1.10 (m, 20H), 0.88 (t, J = 6.9 Hz, 3H). ^{13}C-NMR (101 MHz, $CDCl_3$, ppm): δ 172.2, 130.2, 129.8, 123.2 (q, J = 277.2 Hz), 60.3 (q, J = 36.5 Hz), 33.8, 32.1, 30.0–29.0 (8C), 27.4, 27.3, 24.9, 22.8, 14.2. ^{19}F-NMR (470 MHz, $CDCl_3$, ppm) δ −73.90 (t, J = 8.3 Hz). NMR spectra are shown in Figures S19–S21.

DH-HDPE

The procedure was adapted from a reported method.[4] In a nitrogen-filled glovebox, HDPE (100 mg, 3.56 mmol, 1.0 equiv), Ir-*t*BuPOCOP (9.8 mg, 15 μmol, 0.0042 equiv), NaO*t*Bu (1.6 mg, 16 μmol, 0.0046 equiv), 3,3-dimethyl-1-butene (150 mg, 1.78 mmol, 0.5 equiv), and 3 mL xylene were charged to an oven-dried Schlenk tube. The Schlenk tube was taken out from the glovebox and heated at 200°C for 12 h. The mixture was then poured into 100 mL acetone, and the precipitate was collected and dried without further purification. ^{1}H-NMR spectra for DH-HDPE are shown in Figures S22 and S23.

PDCPD

Dicyclopentadiene, 10 mL, was heated to 45°C. During vigorous stirring, 3.2 mg Grubbs second-generation catalyst in 100 μL DCM was added to the dicyclopentadiene. The mixture was quickly transferred to a Petri dish. After the mixture was solidified, it was heated in an oven at 80°C for 30 min. After cooling down, the resulting PDCPD was cut into pieces and subjected to a Retsch CryoMill for ball mill grinding.

SUPPLEMENTAL INFORMATION

Supplemental information can be found online at https://doi.org/10.1016/j.xcrp.2024.102104.

ACKNOWLEDGMENTS

This material is based upon work supported by University of Akron and the National Science Foundation under grant no. DMR-2042494. H.C. acknowledges a Robert E. Helm Fellowship for financial support. We thank C. Bochenek and C. Wesdemiotis for the mass spectrometry analysis, and the mass spectrometry experiments were supported by the National Science Foundation under grant no. DMR-2215940. We thank A.N. Pathan and J.M. Eagan for the HT-GPC analysis. J.W. acknowledges the Alfred P. Sloan Foundation for a Sloan Research Fellowship (FG-2023-20341).

AUTHOR CONTRIBUTIONS

Conceptualization, H.C. and J.W.; methodology, H.C. and J.W.; validation, X.G.; investigation, H.C., X.G., P.Z., and D.S.; writing – original draft, H.C.; writing – review & editing, X.G. and J.W. Supervision, J.W.

DECLARATION OF INTERESTS

J.W. and H.C. are inventors on US provisional patent application 63/645,410 that covers photo-mediated oxidative degradation of unsaturated polymers.

Received: December 14, 2023
Revised: May 31, 2024
Accepted: June 20, 2024
Published: July 12, 2024

REFERENCES

1. Geyer, R., Jambeck, J.R., and Law, K.L. (2017). Production, Use, and Fate of All Plastics Ever Made. Sci. Adv. *3*, e1700782. https://doi.org/10.1126/sciadv.1700782.

2. Law, K.L., and Narayan, R. (2021). Reducing Environmental Plastic Pollution by Designing Polymer Materials for Managed End-of-Life. Nat. Rev. Mater. *7*, 104–116. https://doi.org/10.1038/s41578-021-00382-0.

3. Arroyave, A., Cui, S., Lopez, J.C., Kocen, A.L., LaPointe, A.M., Delferro, M., and Coates, G.W. (2022). Catalytic Chemical Recycling of Post-Consumer Polyethylene. J. Am. Chem. Soc. *144*, 23280–23285. https://doi.org/10.1021/jacs.2c11949.

4. Conk, R.J., Hanna, S., Shi, J.X., Yang, J., Ciccia, N.R., Qi, L., Bloomer, B.J., Heuvel, S., Wills, T., Su, J., et al. (2022). Catalytic Deconstruction of Waste Polyethylene with Ethylene to Form Propylene. Science *377*, 1561–1566. https://doi.org/10.1126/science.add1088.

5. Wang, N.M., Strong, G., DaSilva, V., Gao, L., Huacuja, R., Konstantinov, I.A., Rosen, M.S., Nett, A.J., Ewart, S., Geyer, R., et al. (2022). Chemical Recycling of Polyethylene by Tandem Catalytic Conversion to Propylene. J. Am. Chem. Soc. *144*, 18526–18531. https://doi.org/10.1021/jacs.2c07781.

6. Gupte, S.L., and Madras, G. (2004). Catalytic Degradation of Polybutadiene. Polym. Degrad. Stab. *86*, 529–533. https://doi.org/10.1016/j.polymdegradstab.2004.06.006.

7. Liu, P., and Ai, C. (2018). Olefin Metathesis Reaction in Rubber Chemistry and Industry and Beyond. Ind. Eng. Chem. Res. *57*, 3807–3820. https://doi.org/10.1021/acs.iecr.7b03830.

8. Rabek, J.F., Lucki, J., and Rånby, B. (1979). Comparative Studies of Reactions of Commercial Polymers with Molecular Oxygen, Singlet Oxygen, Atomic Oxygen and Ozone—I. Reactions with Cis-1,4-Polybutadiene. Eur. Polym. J. *15*, 1089–1100. https://doi.org/10.1016/0014-3057(79)90042-9.

9. Berto, P., Grelier, S., Peruch, F., and Peruch, F. (2018). Controlled Degradation of Polyisoprene and Polybutadiene: A Comparative Study of Two Methods. Polym. Degrad. Stab. *154*, 295–303. https://doi.org/10.1016/j.polymdegradstab.2018.06.019.

10. Rooshenass, P., Yahya, R., and Gan, S.N. (2018). Preparation of Liquid Epoxidized Natural Rubber by Oxidative Degradations Using Periodic Acid, Potassium Permanganate and UV-Irradiation. J. Polym. Environ. *26*, 1378–1392. https://doi.org/10.1007/s10924-017-1038-x.

11. Sadaka, F., Campistron, I., Laguerre, A., and Pilard, J.-F. (2012). Controlled Chemical Degradation of Natural Rubber Using Periodic Acid: Application for Recycling Waste Tyre Rubber. Polym. Degrad. Stab. *97*, 816–828. https://doi.org/10.1016/j.polymdegradstab.2012.01.019.

12. Liu, Y., Tang, Z., Chen, J., Xiong, J., Wang, D., Wang, S., Wu, S., and Guo, B. (2020). Tuning the Mechanical and Dynamic Properties of Imine Bond Crosslinked Elastomeric Vitrimers by Manipulating the Crosslinking Degree. Polym. Chem. *11*, 1348–1355. https://doi.org/10.1039/C9PY01826C.

13. Rahmatpanah, Z., and Alavi Nikje, M.M. (2021). A Novel Synthesis of Polybutadiene-Based Polyurethane Binder and Conductive Graphene–Polyurethane Nanocomposites: a New Approach to Polybutadiene Recycling. Polym. Bull. *78*, 3651–3666. https://doi.org/10.1007/s00289-020-03288-z.

14. Xu, L., Jie, S., Bu, Z., and Li, B.-G. (2021). Preparation of Primary Amine-Terminated Polybutadiene from Cis-Polybutadiene. Eur. Polym. J. *152*, 110484. https://doi.org/10.1016/j.eurpolymj.2021.110484.

15. Gardette, M., Perthué, A., Gardette, J.L., Janecska, T., Földes, E., Pukánszky, B., and Therias, S. (2013). Photo- and Thermal-Oxidation of Polyethylene: Comparison of Mechanisms and Influence of Unsaturation Content. Polym. Degrad. Stab. *98*, 2383–2390. https://doi.org/10.1016/j.polymdegradstab.2013.07.017.

16. Claus, H. (2021). Ozone Generation by Ultraviolet Lamps. Photochem. Photobiol. *97*, 471–476. https://doi.org/10.1111/php.13391.

17. Bradbury, J.H., and Perera, M.C.S. (1988). Advances in the Epoxidation of Unsaturated Polymers. Ind. Eng. Chem. Res. *27*, 2196–2203. https://doi.org/10.1021/ie00084a001.

18. Ogino, T., and Kikuiri, N. (1989). Homogeneous Permanganate Oxidation in Nonaqueous Organic Solution. 4. Evidence for the Existence of the Metastable Manganate(V) Ester Intermediate in the Permanganate Oxidation of Endo-Dicylopentadiene. J. Am. Chem. Soc. *111*, 6174–6177. https://doi.org/10.1021/ja00198a030.

19. Keller, R.W. (1985). Oxidation and Ozonation of Rubber. Rubber Chem. Technol. *58*, 637–652. https://doi.org/10.5254/1.3536082.

20. Gardette, J.-L., and Lemaire, J. (1991). Photothermal and Thermal Oxidations of Rigid, Plasticized and Pigmented Poly(vinyl chloride). Polym. Degrad. Stab. *34*, 135–167. https://doi.org/10.1016/0141-3910(91)90117-A.

21. Bussière, P.O., Gardette, J.L., Lacoste, J., and Baba, M. (2005). Characterization of Photodegradation of Polybutadiene and Polyisoprene: Chronology of Crosslinking and Chain-Scission. Polym. Degrad. Stab. *88*, 182–188. https://doi.org/10.1016/j.polymdegradstab.2004.02.013.

22. Smith, L.M., Aitken, H.M., and Coote, M.L. (2018). The Fate of the Peroxyl Radical in Autoxidation: How Does Polymer Degradation Really Occur? Acc. Chem. Res. *51*, 2006–2013. https://doi.org/10.1021/acs.accounts.8b00250.

23. Aldas, M., Paladines, A., Valle, V., Pazmiño, M., and Quiroz, F. (2018). Effect of the Prodegradant-Additive Plastics Incorporated on the Polyethylene Recycling. Int. J. Polym. Sci. *2018*, 1–10. https://doi.org/10.1155/2018/2474176.

24. Tawfic, M.L., Morsi, M., and Shafik, E.S. (2022). Natural Abundant Prodegradant for Oxo-Degradation of Polymers. J. Polym. Res. *29*, 60. https://doi.org/10.1007/s10965-022-02907-9.

25. Braaz, R., Armbruster, W., and Jendrossek, D. (2005). Heme-Dependent Rubber Oxygenase RoxA of Xanthomonas sp. Cleaves the Carbon Backbone of Poly(cis-1,4-Isoprene) by a Dioxygenase Mechanism. Appl. Environ. Microbiol. *71*, 2473–2478. https://doi.org/10.1128/AEM.71.5.2473-2478.2005.

26. Cristina Silva Costa, D. (2020). Additions to Non-Activated Alkenes: Recent Advances. Arab. J. Chem. *13*, 799–834. https://doi.org/10.1016/j.arabjc.2017.07.017.

27. Sahu, S., and Goldberg, D.P. (2016). Activation of Dioxygen by Iron and Manganese Complexes: A Heme and Nonheme Perspective. J. Am. Chem. Soc. *138*, 11410–11428. https://doi.org/10.1021/jacs.6b05251.

28. Huang, Z., Guan, R., Shanmugam, M., Bennett, E.L., Robertson, C.M., Brookfield, A., McInnes, E.J.L., and Xiao, J. (2021). Oxidative Cleavage of Alkenes by O2 with a Non-Heme Manganese Catalyst. J. Am. Chem. Soc. *143*, 10005–10013. https://doi.org/10.1021/jacs.1c05757.

29. Norrish, R.G.W., and Bamford, C.H. (1937). Photo-Decomposition of Aldehydes and Ketones. Nature *140*, 195–196. https://doi.org/10.1038/140195b0.

30. Rollefson, G.K. (1937). The Photochemical Behavior of the Aldehydes. J. Phys. Chem. *41*, 259–265. https://doi.org/10.1021/j150380a008.

31. Carlisle, P.J., and Levine, A.A. (1932). Stability of Chlorohydrocarbons I. Methylene Chloride. Ind. Eng. Chem. *24*, 146–147. https://doi.org/10.1021/ie50266a006.

32. Maltese, F., van der Kooy, F., and Verpoorte, R. (2009). Solvent Derived Artifacts in Natural Products Chemistry. Nat. Prod. Commun. *4*, 447–454. https://doi.org/10.1177/1934578X0900400326.

33. Hufendiek, A., Lingier, S., and Du Prez, F.E. (2019). Thermoplastic Polyacetals: Chemistry from the Past for a Sustainable Future? Polym. Chem. *10*, 9–33. https://doi.org/10.1039/C8PY01219A.

34. Basedow, A.M., Ebert, K.H., and Ederer, H.J. (1978). Kinetic Studies on the Acid Hydrolysis of Dextran. Macromolecules *11*, 774–781. https://doi.org/10.1021/ma60064a031.

35. Bruneel, D., and Schacht, E. (1995). Enzymatic Degradation of Pullulan and Pullulan Derivatives. J. Bioact. Compat Polym. *10*, 299–312. https://doi.org/10.1177/088391159501000402.

36. Tobita, H. (1996). Random Degradation of Branched Polymers. 1. Star Polymers. Macromolecules *29*, 3000–3009. https://doi.org/10.1021/ma950971c.

37. Tayal, A., and Khan, S.A. (2000). Degradation of a Water-Soluble Polymer: Molecular Weight Changes and Chain Scission Characteristics. Macromolecules *33*, 9488–9493. https://doi.org/10.1021/ma000736g.

38. Alder, R.W., and Reddy, B.S.R. (1994). Attempted Equilibration of an Insoluble Spiran Polymer with Monomers and Oligomers through Reversible Chemical Reactions: Transketalization Route to Spiropolymers from 1,4-Cyclohexanedione and Pentaerythritol. Polymer *35*, 5765–5772. https://doi.org/10.1016/S0032-3861(05)80054-0.

39. Heffernan, M.J., and Murthy, N. (2005). Polyketal Nanoparticles: A New pH-Sensitive Biodegradable Drug Delivery Vehicle. Bioconjug. Chem. *16*, 1340–1342. https://doi.org/10.1021/bc050176w.

40. Fiore, V.F., Lofton, M.C., Roser-Page, S., Yang, S.C., Roman, J., Murthy, N., and Barker, T.H. (2010). Polyketal Microparticles for Therapeutic Delivery to the Lung. Biomaterials *31*, 810–817. https://doi.org/10.1016/j.biomaterials.2009.09.100.

41. Moreno, A., Morsali, M., and Sipponen, M.H. (2021). Catalyst-Free Synthesis of Lignin Vitrimers with Tunable Mechanical Properties: Circular Polymers and Recoverable Adhesives. ACS Appl. Mater. Interfaces *13*, 57952–57961. https://doi.org/10.1021/acsami.1c17412.

42. Png, Z.M., Zheng, J., Kamarulzaman, S., Wang, S., Li, Z., and Goh, S.S. (2022). Fully Biomass-Derived Vitrimeric Material with Water-Mediated Recyclability and Monomer Recovery. Green Chem. *24*, 5978–5986. https://doi.org/10.1039/D2GC01556K.

43. Shieh, P., Zhang, W., Husted, K.E.L., Kristufek, S.L., Xiong, B., Lundberg, D.J., Lem, J., Veysset, D., Sun, Y., Nelson, K.A., et al. (2020). Cleavable Comonomers Enable Degradable, Recyclable Thermoset Plastics. Nature *583*, 542–547. https://doi.org/10.1038/s41586-020-2495-2.

44. Sullivan, K.P., Werner, A.Z., Ramirez, K.J., Ellis, L.D., Bussard, J.R., Black, B.A., Brandner, D.G., Bratti, F., Buss, B.L., Dong, X., et al. (2022). Mixed Plastics Waste Valorization through Tandem Chemical Oxidation and Biological Funneling. Science *378*, 207–211. https://doi.org/10.1126/science.abo4626.

45. Korpusik, A.B., Adili, A., Bhatt, K., Anatot, J.E., Seidel, D., and Sumerlin, B.S. (2023). Degradation of Polyacrylates by One-Pot Sequential Dehydrodecarboxylation and Ozonolysis. J. Am. Chem. Soc. *145*, 10480–10485. https://doi.org/10.1021/jacs.3c02497.

46. Wang, K., Jia, R., Cheng, P., Shi, L., Wang, X., and Huang, L. (2023). Highly Selective Catalytic Oxi-Upcycling of Polyethylene to Aliphatic Dicarboxylic Acid under a Mild Hydrogen-Free Process. Angew. Chem. Int. Ed. *62*, e202301340. https://doi.org/10.1002/anie.202301340.

47. Han, Q.-Y., Zhao, C.-L., Yang, J., and Zhang, C.-P. (2017). A Facile 2,2,2-Trifluoroethyl Fatty Acid Ester Synthesis with Phenyl(2,2,2-Trifluoroethyl)iodonium Triflate at Room Temperature. Green Chem. Lett. Rev. *10*, 162–170. https://doi.org/10.1080/17518253.2017.1338759.

Cell Reports Physical Science, Volume *5*

Supplemental information

Deconstruction of unsaturated polymers through photo-mediated oxidation under O_2

Hanlin Chen, Xin Guan, Puyan Zhang, Devavrat Sathe, and Junpeng Wang

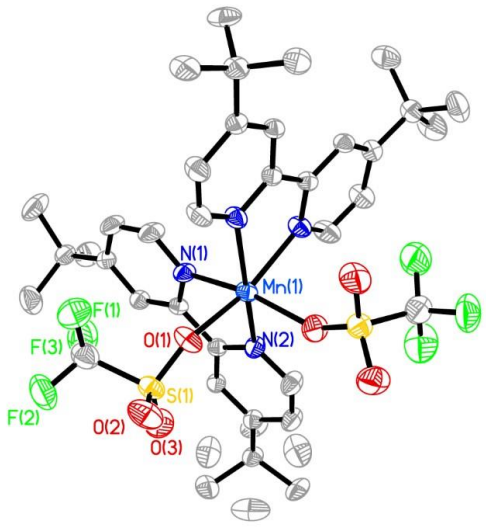

Figure S1. Molecular structure of $Mn(dtbyp)_2(OTf)_2$ from single crystal X-ray diffraction.

Table S1. Crystal data and structure refinement for $Mn(dtbyp)_2(OTf)_2$

Identification code	pbcn_a	
Empirical formula	C38 H48 F6 Mn N4 O6 S2	
Formula weight	889.86	
Temperature	296(2) K	
Wavelength	0.71073 Å	
Crystal system	Orthorhombic	
Space group	Pbcn	
Unit cell dimensions	a = 18.457(2) Å	a= 90°.
	b = 10.9833(14) Å	b= 90°.
	c = 20.845(3) Å	g = 90°.
Volume	4225.8(9) $Å^3$	
Z	4	
Density (calculated)	1.399 Mg/m^3	
Absorption coefficient	0.486 mm^{-1}	
F(000)	1852	
Theta range for data collection	1.954 to 28.315°.	
Index ranges	-24<=h<=24, -14<=k<=0, 0<=l<=27	
Reflections collected	10084	
Independent reflections	5253 [R(int) = 0.0498]	
Completeness to theta = 25.242°	99.9 %	
Absorption correction	None	
Refinement method	Full-matrix least-squares on F^2	
Data / restraints / parameters	5253 / 0 / 292	
Goodness-of-fit on F^2	1.066	
Final R indices [I>2sigma(I)]	R1 = 0.0613, wR2 = 0.1243	
R indices (all data)	R1 = 0.1218, wR2 = 0.1433	
Extinction coefficient	n/a	
Largest diff. peak and hole	0.233 and -0.259 $e.Å^{-3}$	

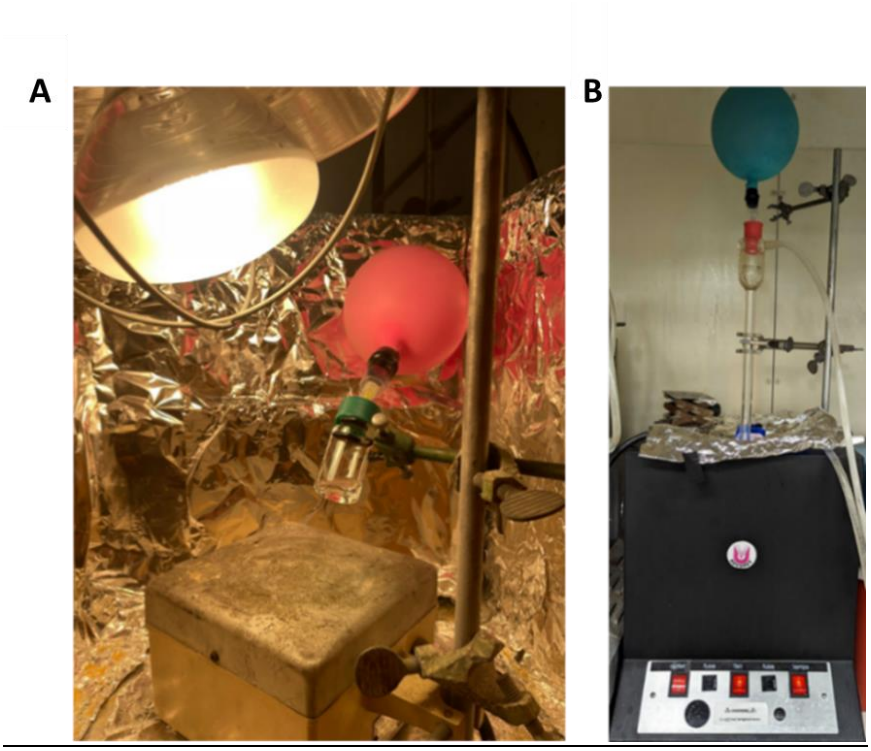

Figure S2. Pictures of the reaction setups with a sunlamp (A) and a Rayonet photoreactor (B). The condenser shown in (B) was only used for gram-scale reactions; for milligram-scale reactions, the balloon was directly connected to the vial.

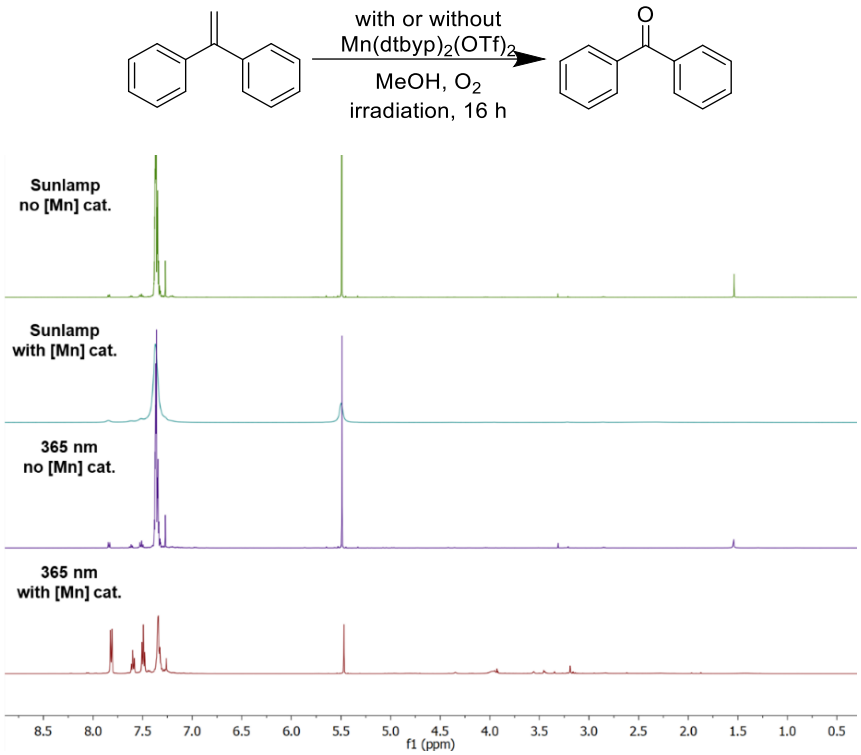

Figure S3. Stacked ^{1}H NMR for photo-mediated oxidation of 1,1-diphenyl ethylene with or without $Mn(dtbypy)_2(OTf)_2$ using a sunlamp or a 365 nm photoreactor.

Table S2. Photo-mediated oxidation of 1,1-diphenyl ethylene with or without $Mn(dtbypy)_2(OTf)_2$ using a sunlamp or a 365 nm photoreactor.

Entry	Lamp	catalyst	conversion[a]
1	sunlamp	$Mn(dtbpy)_2(OTf)_2$	6%
2	sunlamp	–	2%
3	365 nm	$Mn(dtbpy)_2(OTf)_2$	50%
4	365 nm	–	4%

[a]Calculated based on the integrations of ^{1}H NMR peaks for unreacted DPE and the generated benzophenone.

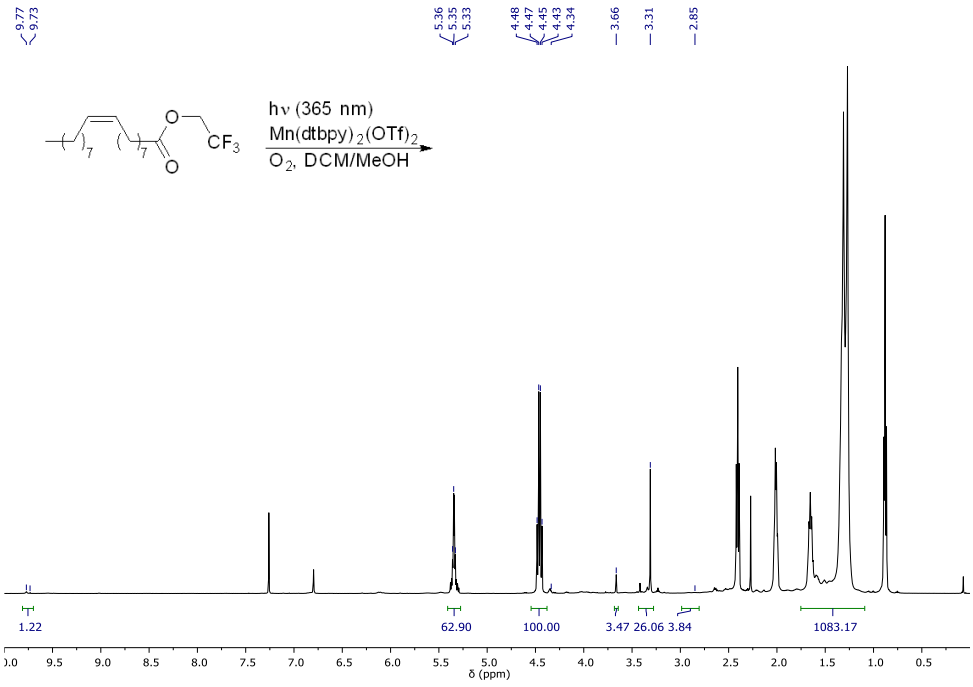

Figure S4. A representative ^{1}H NMR (500 MHz, $CDCl_3$) spectrum for the photo-mediated oxidation of TFO.

Table S3. Conversions of alkene and yields of acetal for the oxidation of TFO in MeOH with various cosolvents.

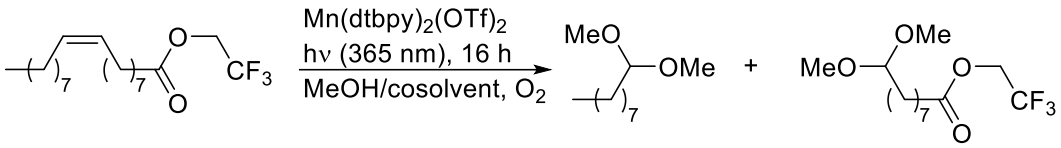

Cosolvent	Conversion (entry1/2/3)	Yield (acetal) (entry1/2/3)
No	16.1% / 15.2% / 14.7%	0.7% / 0.7% / 0.6%
DCM	40.2% / 35.4% / 38.6%	1.6% / 1.3% / 1.4%
$CHCl_3$	22.9% / 23.3% / 23.9%	1.4% / 1.1% / 1.2%
THF	0.8% / 0.8% / 1.0%	0% / 0% / 0%

Table S4. Conversions of alkene and yields of acetal for the oxidation of TFO with varied equiv. $Mn(dtbpy)_2(OTf)_2$ catalyst.

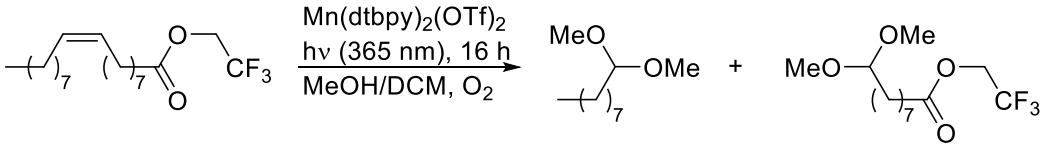

Catalyst loading (equiv.)	Conversion (entry1/2/3)	Yield (acetal) (entry1/2/3)
2.0×10^{-2}	40.4% / 35.1% / 37.5%	2.9% / 2.8% / 2.8%
1.0×10^{-2}	37.0% / 32.8% / 33.4%	1.3% / 1.2% / 1.2%
5.0×10^{-3}	27.0% / 27.9% / 27.1%	0.5% / 0.7% / 0.5%
1.0×10^{-3}	17.4% / 19.2% / 17.9%	0% / 0% / 0%
5.0×10^{-4}	13.1% / 15.1% / 14.2%	0% / 0% / 0%
1.0×10^{-4}	6.9% / 8.4% / 7.1%	0% / 0% / 0%

Table S5. Conversions of alkene and yields of acetal for the oxidation of TFO at varied initial concentrations of TFO.

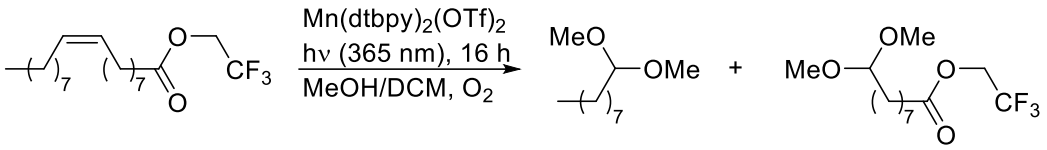

$[TFO]_0$	Conversion (entry1/2/3)	Yield (acetal) (entry1/2/3)
1.0	1.5% / 0% / 0%	0% / 0% / 0%
0.5	17.0% / 14.5% / 15.8%	0.2% / 0.1% / 0.1%
0.25	35.7% / 39.0% / 35.5%	1.7% / 1.3% / 1.4%
0.1	28.0% / 28.6% / 27.1%	1.5% / 1.6% / 1.7%

Table S6. Conversions of alkene and yields of acetal for the oxidation of TFO with or without stabilizer.

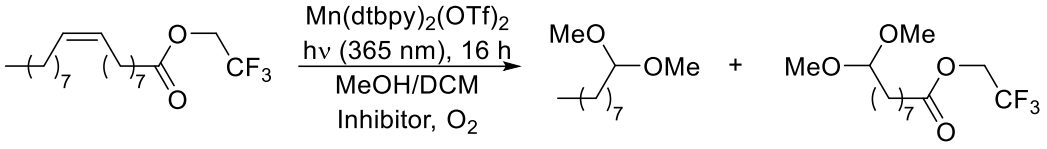

Inhibitor	Conversion (entry1/2/3)	Yield (acetal) (entry1/2/3)	Yield/Conversion (avg.)
No	35.7% / 39.0% / 35.5%	1.7% / 1.3% / 1.4%	3.9%
BHT	30.3% / 35.0% / 28.5%	1.9% / 2.1% / 1.1%	5.4%
VE	32.8% / 35.8% / 36.7%	1.1% / 1.2% / 1.3%	3.4%

Table S7. Conversions of alkene and yields of acetal for the oxidation of TFO with various amount of BHT.

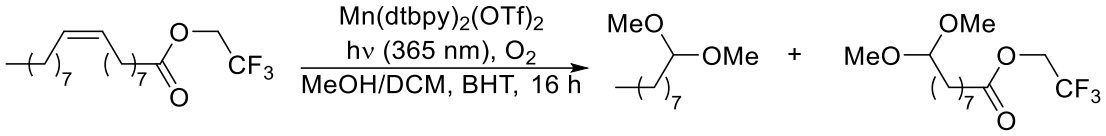

BHT (equiv.)	Conversion (entry1/2/3)	Yield (acetal) (entry1/2/3)
0.03	35.0% / 35.4% / 30.2%	1.6% / 2.2% / 1.5%
0.01	32.2% / 34.4% / 33.6%	1.7% / 1.7% / 1.6%
0.003	34.2% / 37.2% / 33.4%	1.2% / 2.2% / 1.3%
0.001	30.3% / 35.0% / 28.5%	1.9% / 2.1% / 1.1%
3.0×10^{-4}	34.5% / 35.3% / 37.4%	1.9% / 2.4% / 1.5%
1.0×10^{-4}	34.2% / 36.0% / 39.2%	1.7% / 2.3% / 1.8%

Table S8. Conversions of alkene and yields of acetal for the oxidation of TFO under pure oxygen and ambient air.

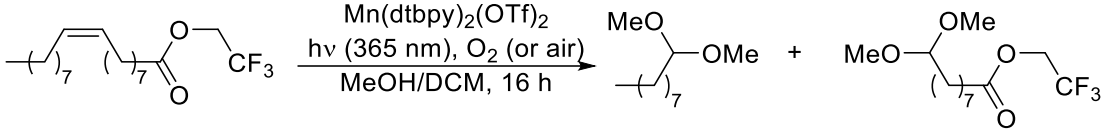

Atmosphere	Conversion (entry1/2/3)	Yield (acetal) (entry1/2/3)	Yield/Conversion (avg.)
Pure oxygen	35.7% / 39.0% / 35.5%	1.7% / 1.3% / 1.4%	3.9%
Ambient air	14.3% / 15.2% / 13.4%	0.6% / 0.6% / 0.4%	3.7%

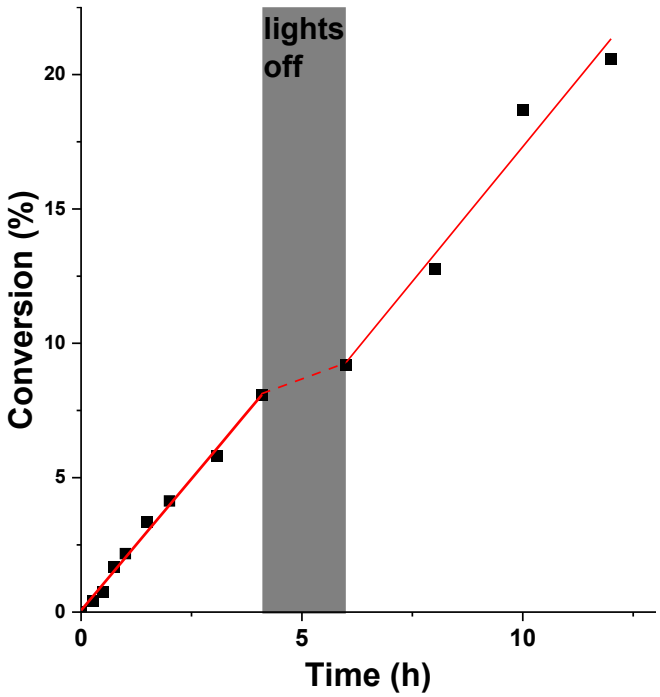

Figure S5. Photo-mediated oxidation of TFO under the optimized condition (1 mol% $Mn(dtbpy)_2(OTf)_2$, 0.3 mol% BHT, $[TFO]_0$ = 0.25 M, DCM/MeOH v/v 9/1), 1 atm O_2, 365 nm irradiation at room temperature) when lights were on for 4 h, off for 2 h, and then on for 6 h.

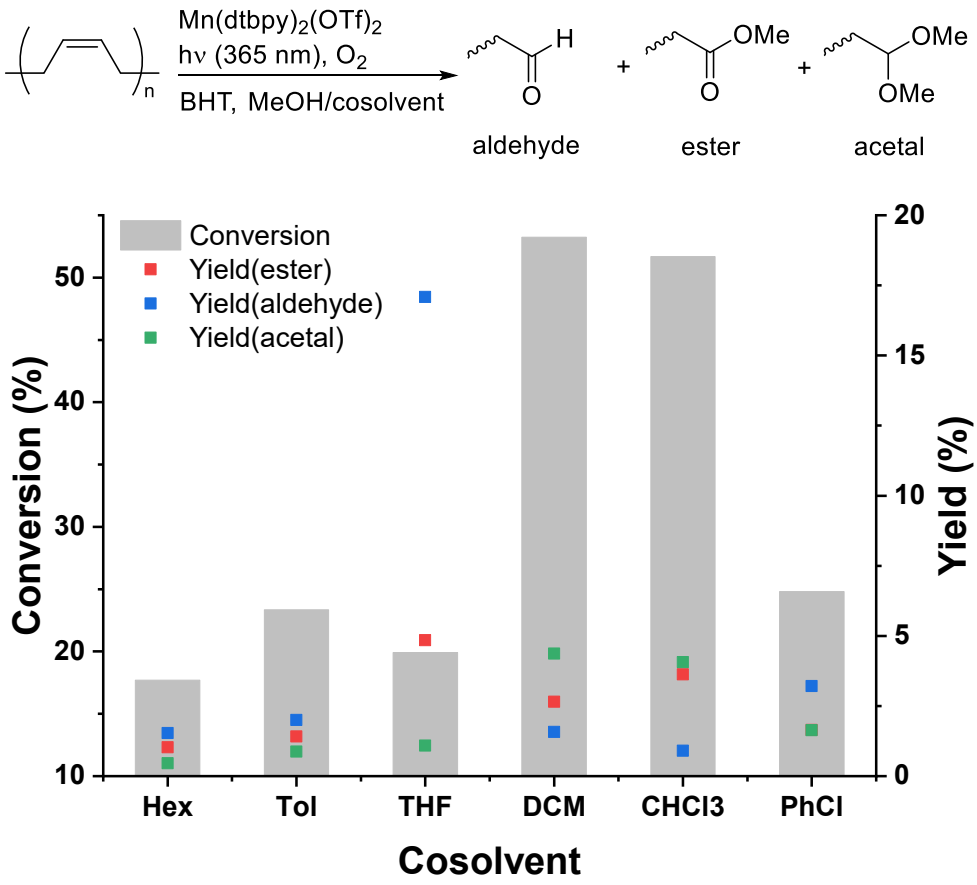

Figure S6. Photo-mediated oxidative degradation of PB in MeOH with various cosolvents under the following conditions: 1 mol% $Mn(dtbpy)_2(OTf)_2$, 0.3 mol% BHT, $[TFO]_0$ = 0.25 M, cosolvent/MeOH (9/1), 1 atm O_2, 365 nm irradiation at room temperature.

Table S9. Conversions of alkene and yields of acetal for the oxidation of PB at varied numbers of lamps.

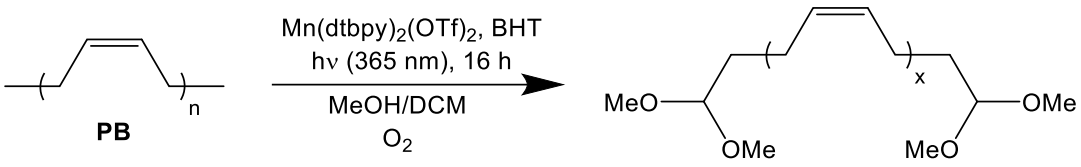

Number of lamps	Conversion (entry1/2/3)	Yield (acetal) (entry1/2/3)
4	15.4% / 21.4% / 15.1%	0.3% / 0.6% / 0.6%
8	39.2% / 47.3% / 45.3%	2.9% / 2.3% / 2.2%
16	64.7% / 58.7% / 51.6%	5.6% / 3.8% / 3.0%

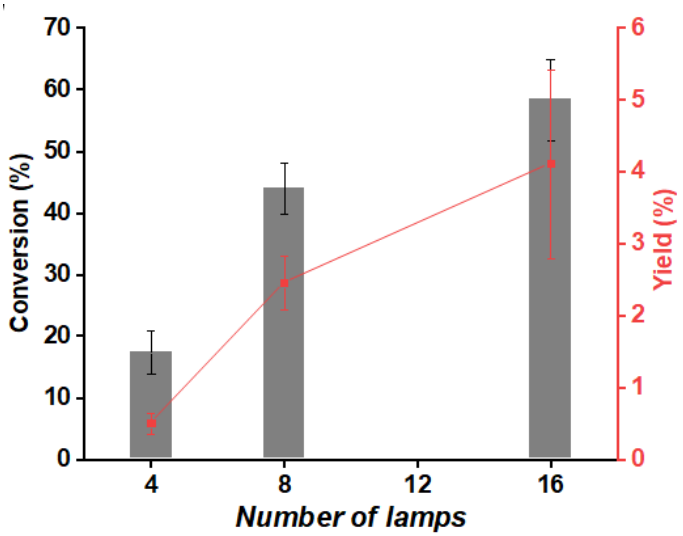

Figure S7. Effect of light intensity on the photo-mediated oxidative degradation of PB. Condition: 1 mol% $Mn(dtbpy)_2(Otf)_2$, 0.3 mol% BHT, 13.5 mg PB ($[alkene]_0$ = 0.25 M), MeOH/DCM (1:9), 1 atm oxygen, irradiation with different numbers of lamps of 365 nm wavelength at room temperature.

Table S10. Conversions of alkene and yields of acetal for the oxidation of PB with various amounts of BHT.

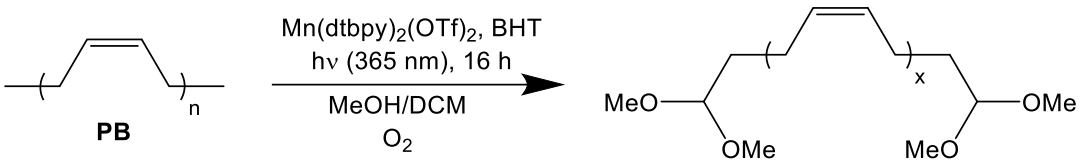

BHT (equiv.)	Conversion (entry1/2/3)	Yield (acetal) (entry1/2/3)
0.03	58.0% / 44.9% / 49.4%	3.2% / 2.4% / 3.0%
0.01	56.5% / 56.1% / 57.5%	5.2% / 3.6% / 3.5%
0.003	64.7% / 58.7% / 51.6%	5.6% / 3.8% / 3.0%
0.001	63.4% / 55.6% / 56.4%	4.3% / 3.3% / 3.3%
3.0×10^{-4}	63.2% / 60.6% / 62.7%	4.3% / 3.9% / 3.3%
1.0×10^{-4}	47.7% / 59.0% / 58.3%	3.2% / 4.2% / 3.6%

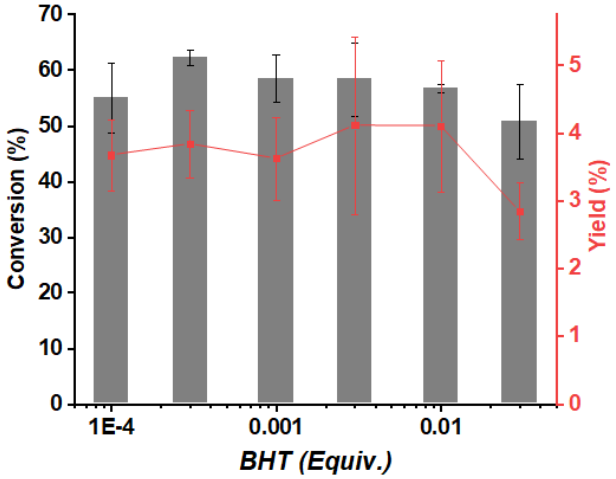

Figure S8. Effect of BHT loading on the photo-mediated oxidative degradation of PB (1 mol% $Mn(dtbpy)_2(Otf)_2$, 13.5 mg PB ($[alkene]_0$ = 0.25 M), MeOH/DCM (1:9), 1 atm oxygen, 365 nm irradiation at room temperature).

Table S11. Conversions of alkene and yields of acetal for the oxidation of PB under air.

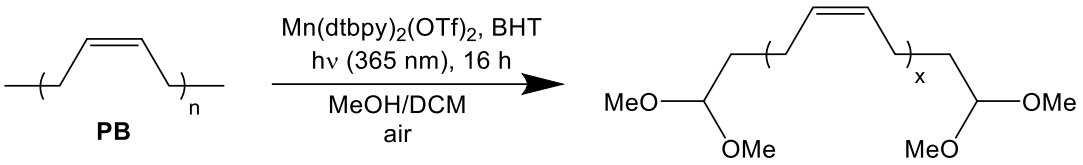

Atmosphere	Conversion	Yield (acetal)
Ambient air	13.0%	1.9%

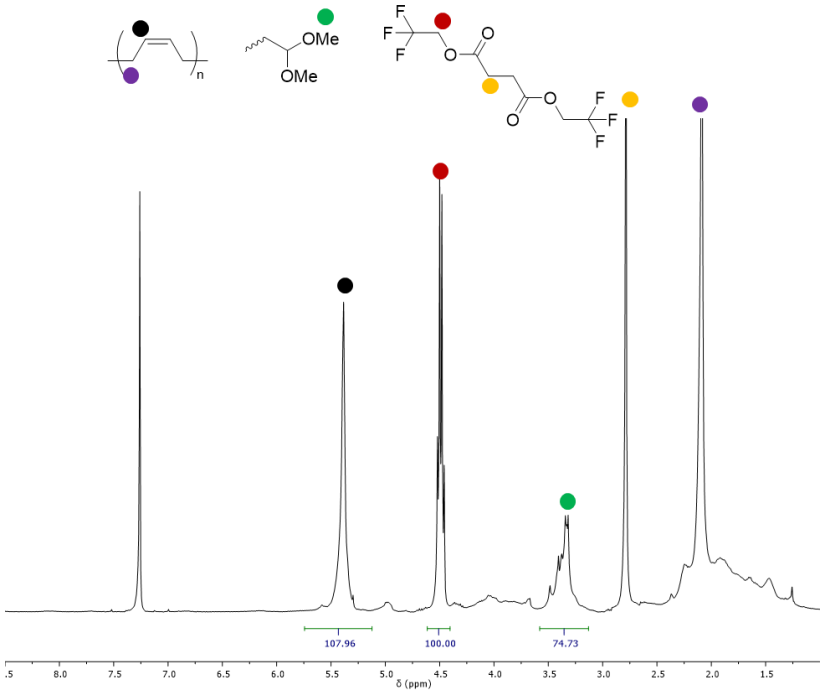

Figure S9. ^{1}H NMR (500 MHz, $CDCl_3$) spectrum for 80 h of photo-mediated oxidative degradation of PB. According to the integrations of the peaks for alkene, internal standard, and acetal, the conversion of alkene is 56.8%, and the yield of acetal is 5.0%.

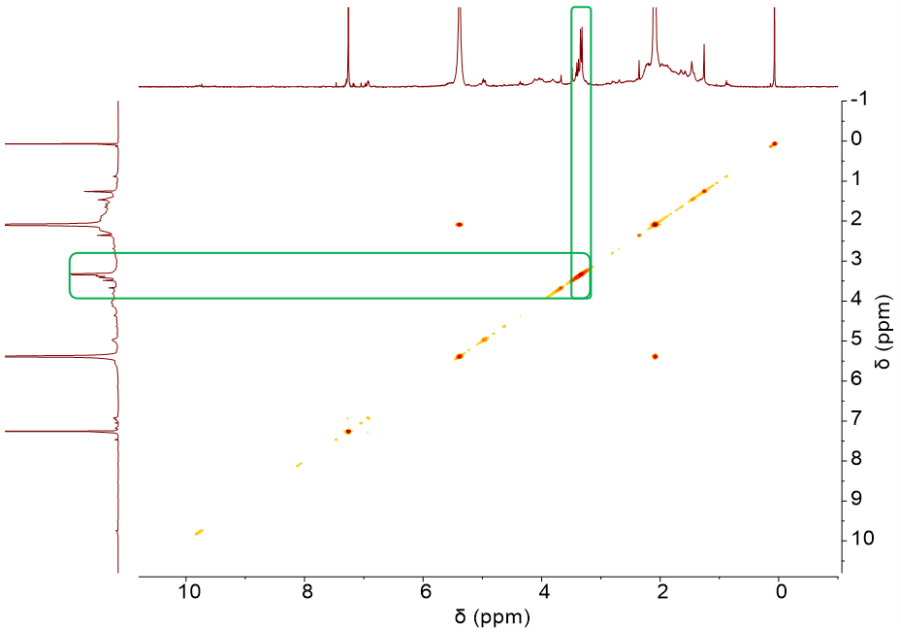

Figure S10. ^{1}H-^{1}H COSY NMR (500 MHz, $CDCl_3$) spectrum for photo-mediated oxidative degradation of PB.

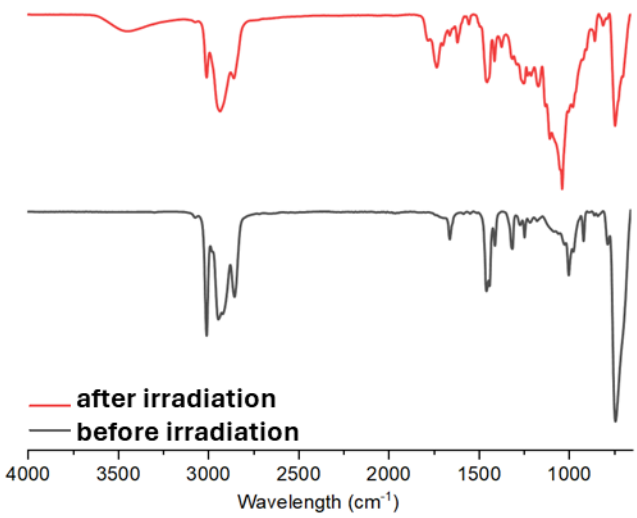

Figure S11. FTIR spectra for PB before (black) and after (red) photo-mediated oxidative degradation.

Table S11. Kinetic data including conversion, number-average molecular weight M_n, and dispersity $Đ$ for the photo-mediated oxidative degradation of PB (Raw data of Figure 4c-d).

Time (h)	Conversion	M_n (kDa)	$Đ$
0	0.0%	149.6	4.88
1	0.3%	144.4	4.86
2	3.0%	136.0	4.64
4	3.2%	136.2	3.73
6	2.8%	120.0	3.39
8	3.1%	107.0	4.15
9	3.3%	102.3	3.30
10	1.8%	92.2	2.69
12	2.8%	32.7	1.99
13	2.4%	20.5	1.89
14	6.0%	15.5	1.80
15	7.0%	15.2	1.82
16	11.3%	13.0	1.99[a]
18	11.5%	10.3	2.04[a]
22	10.5%	5.3	2.34[a]
25	10.1%	4.9	2.28[a]
33.5	24.8%	2.7	3.03[a]
46.75	33.1%	1.5	3.52[a]
57.5	40.9%	0.06[b]	-
70	45.1%	0.10[b]	-
79.5	57.8%	0.04[b]	-
95.25	63.2%	0.03[b]	-
118.25	72.5%	0.03[b]	-

[a]On the GPC trace, the peak of polymer/oligomer overlapped with low molecular weight peak (lower than the calibration limit of 500 Da), which led to an abnormal increase of dispersity. [b]The molecular weight fo the main peak was below the calibration limit of 500 Da.

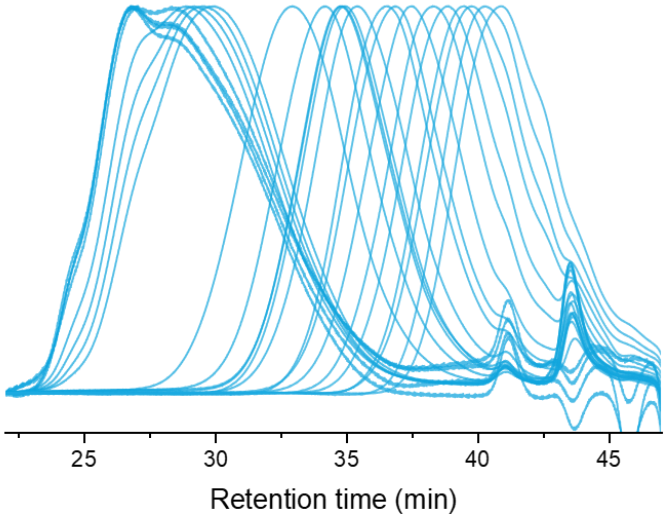

Figure S12. GPC traces for the photo-mediated degradation of PB.

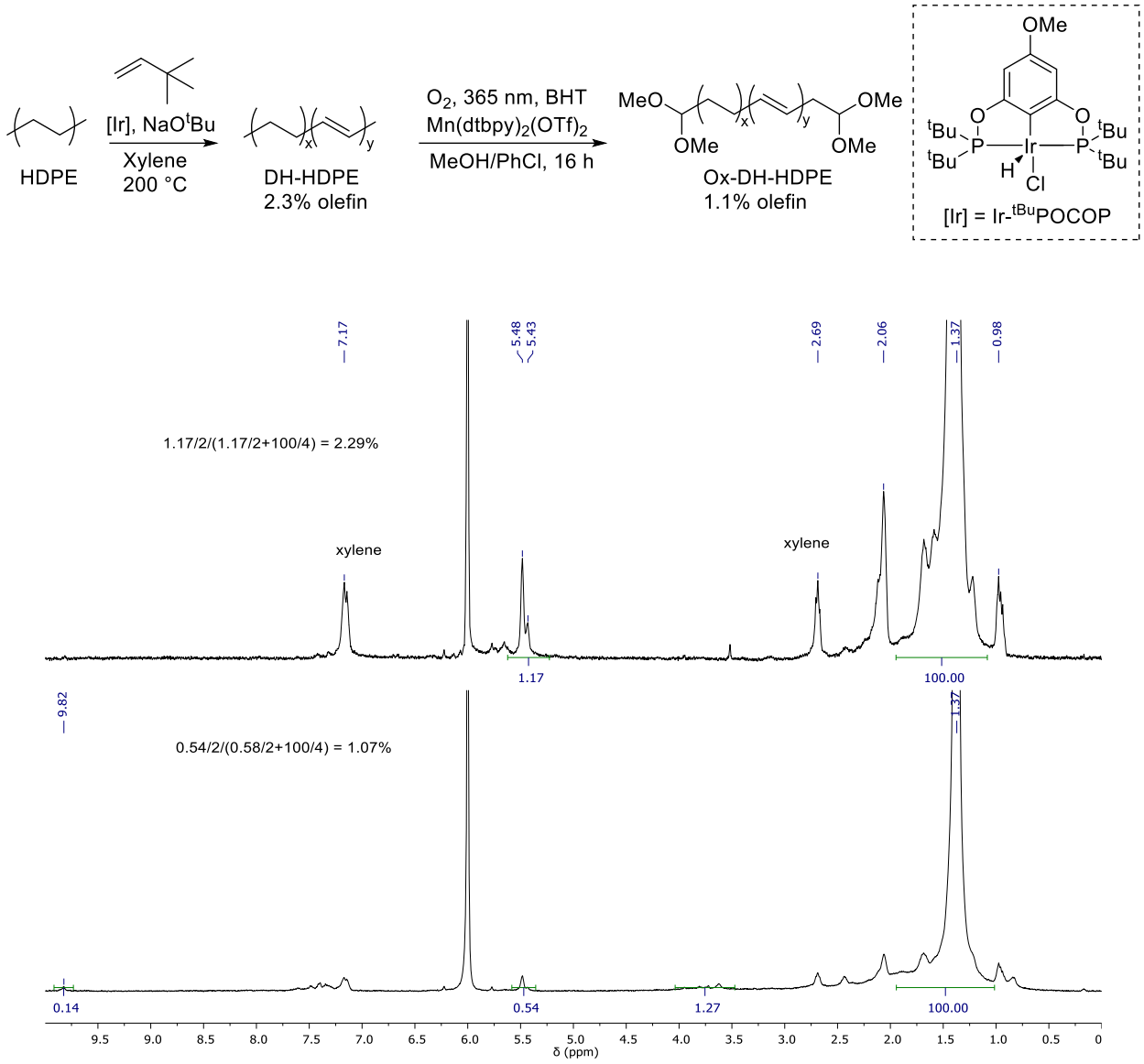

Figure S13. ^{1}H NMR (400 MHz, tetrachloroethane-*d2*) spectrum for the DH-HDPE before (top) and after (bottom) photo-mediated oxidative degradation at room temperature. The amount of olefin decreased from 2.29% to 1.07% after the photo-mediated oxidation and generated 0.84% acetal with respect to all repeating units (ethylene or olefin), suggesting a 36% yield of acetal with respect to the reacted olefins.

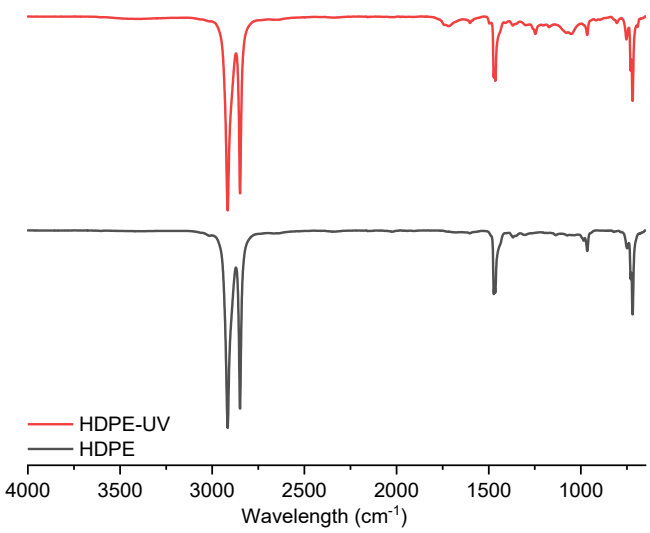

Figure S14. FTIR spectra for DH-HDPE before (black) and after (red) photo-mediated oxidative degradation.

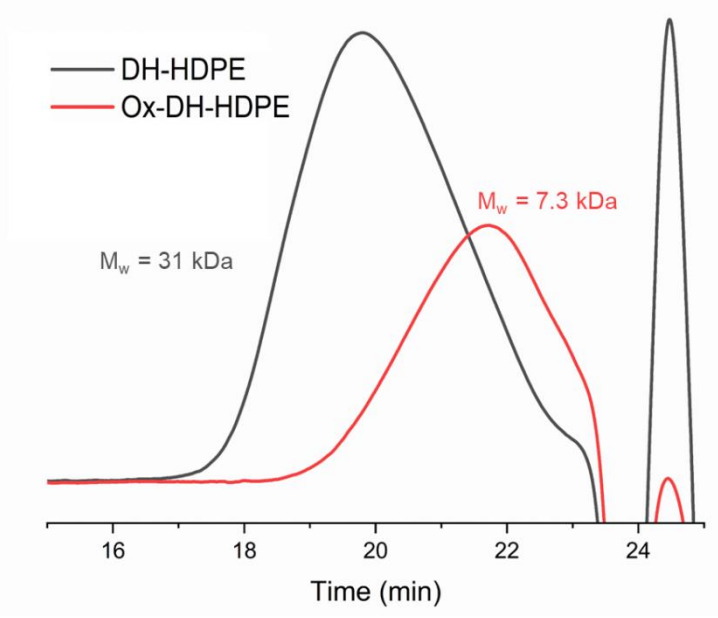

Figure S15. GPC curves for the photo-mediated oxidative cleavage of DH-HDPE (black), and the formed Ox-DH-HDPE (red).

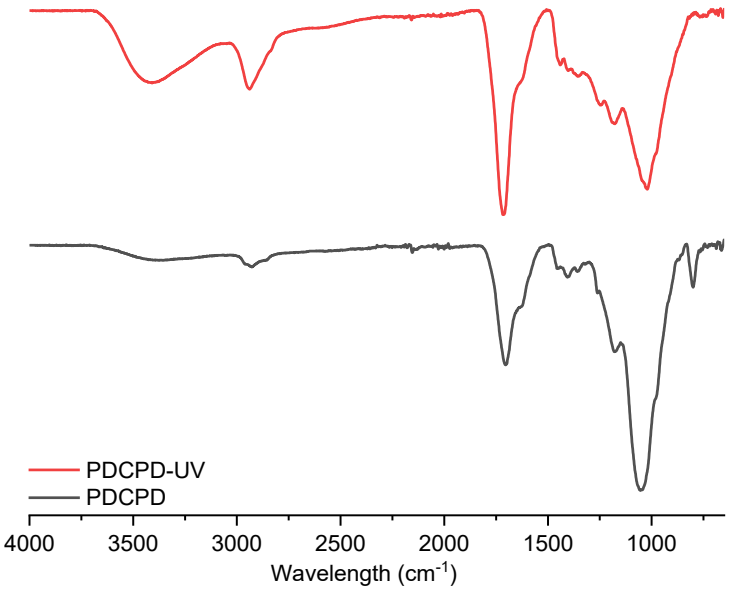

Figure S16. FTIR spectra for PDCPD before (black) and after (red) photo-mediated oxidative degradation.

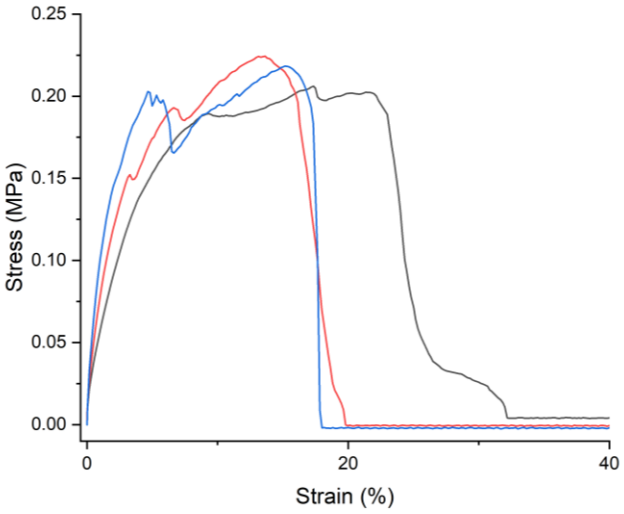

Figure S17. Stress-strain curves obtained from the tensile testing of the polymer network specimens made from the oxidative degradation of PB.

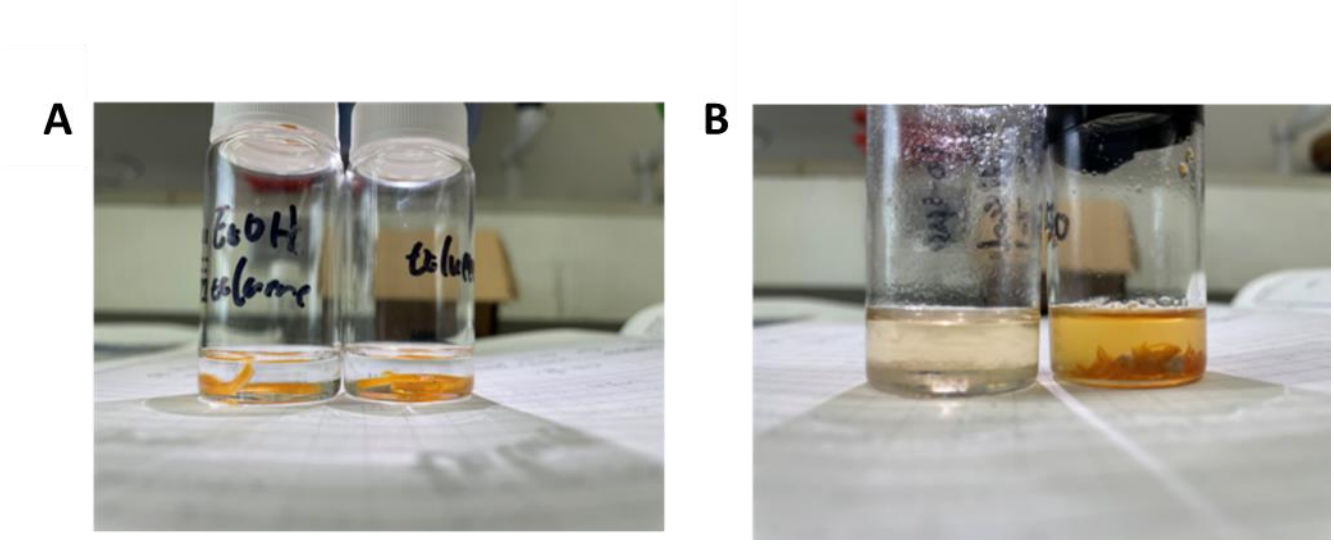

Figure S18. Pictures of vials with polymer network specimens in solvents (6 mL) before (A) and after (B) being heated at 80 °C for 24 h (left vial: in ethanol/toluene 1/2 v/v; right vial: in toluene).

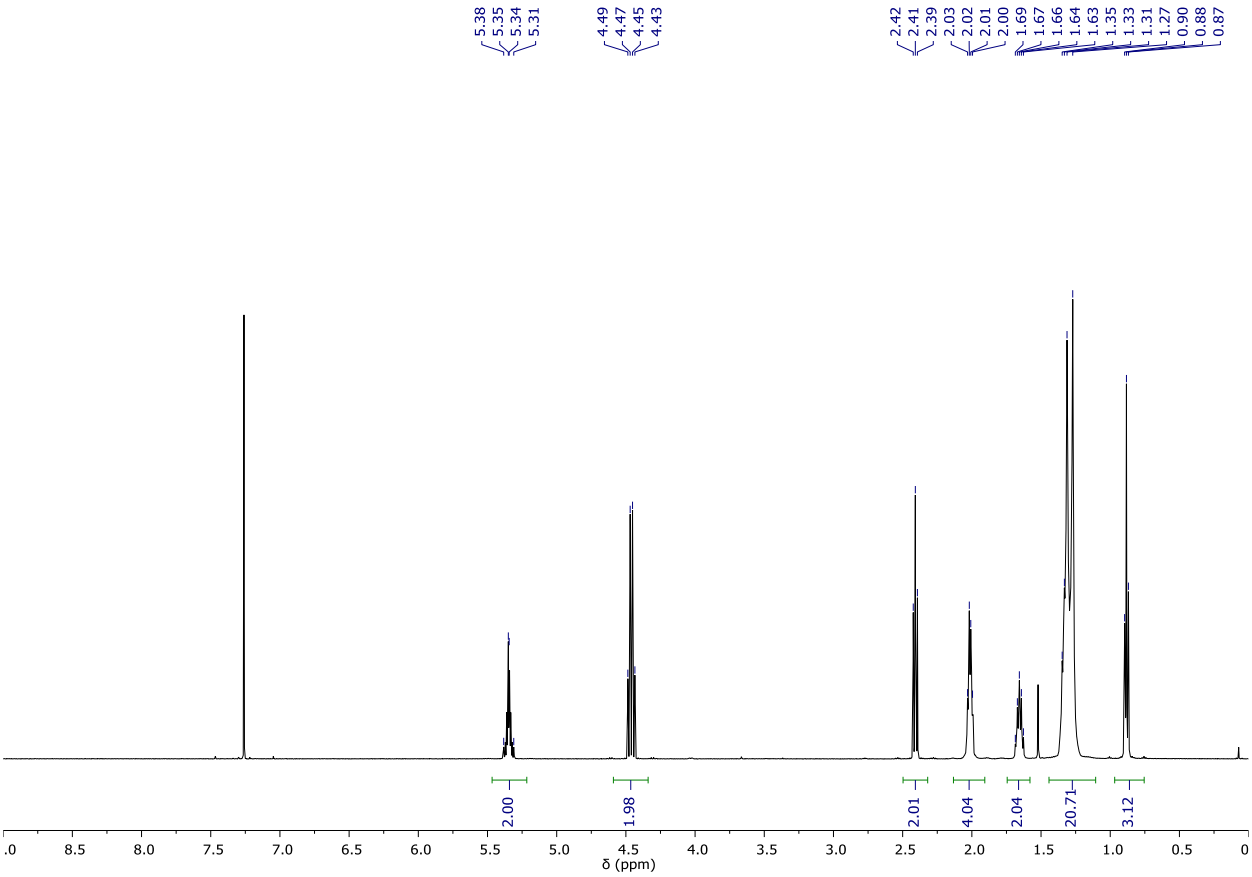

Figure S19. ^{1}H NMR (500 MHz, $CDCl_3$) spectrum for TFO.

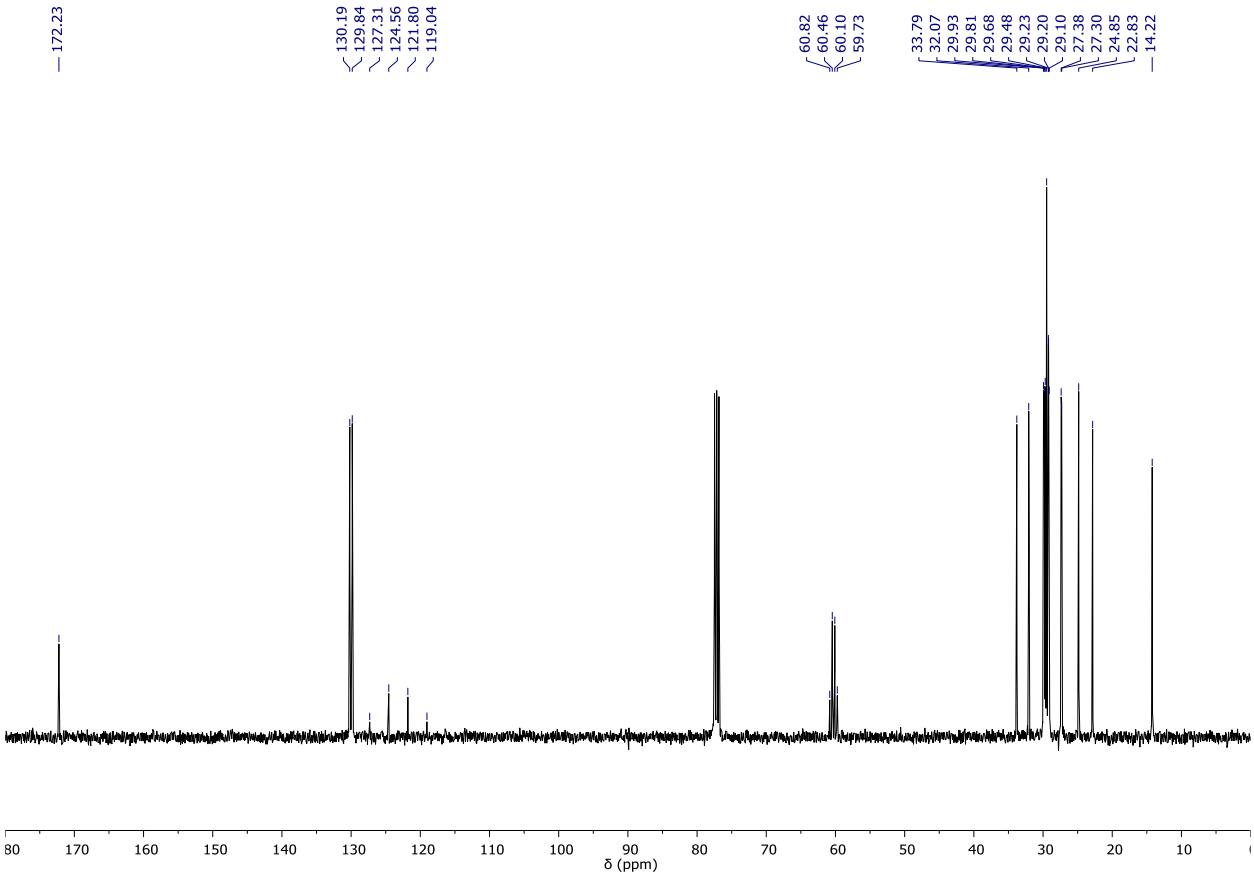

Figure S20. ^{13}C NMR (101 MHz, $CDCl_3$) spectrum for TFO.

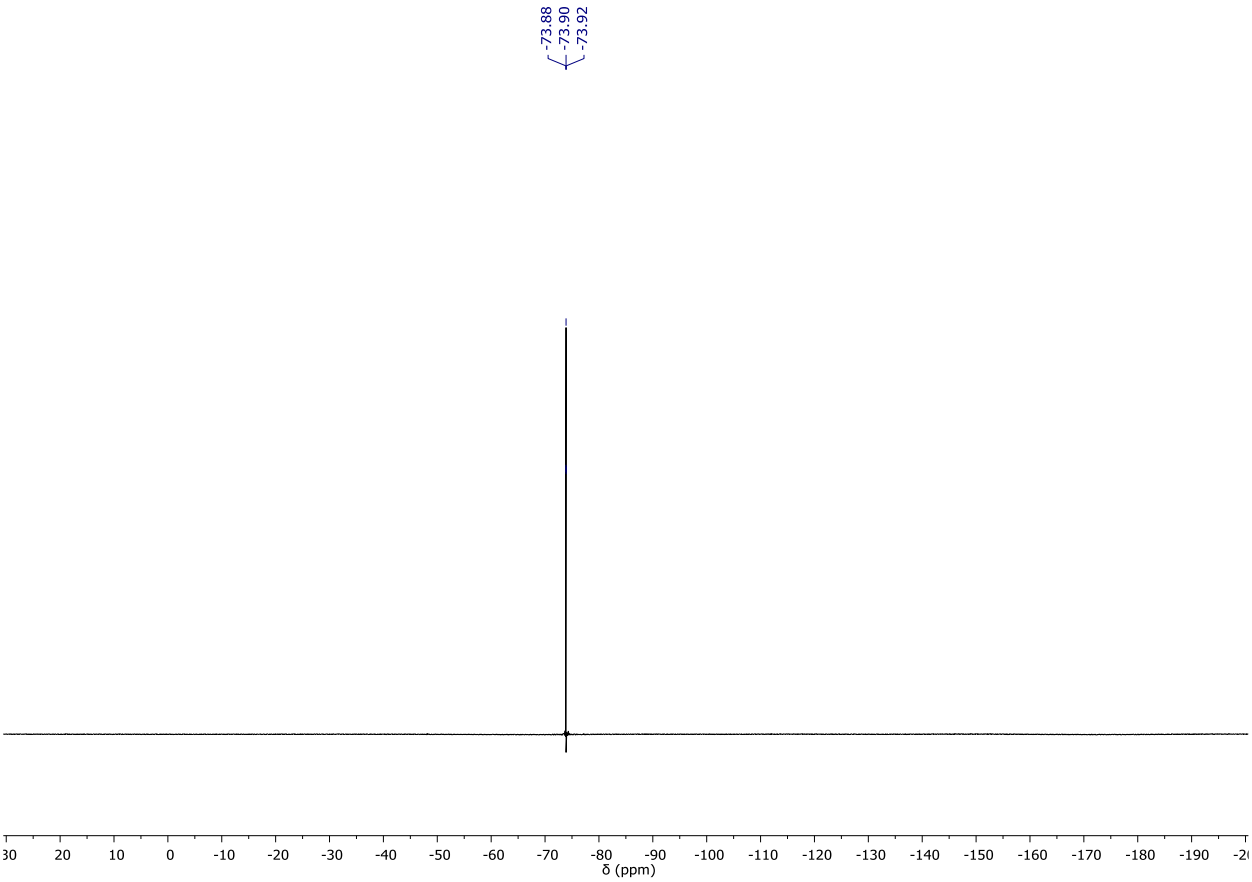

Figure S21. ^{19}F NMR (470 MHz, $CDCl_3$) spectrum for TFO.

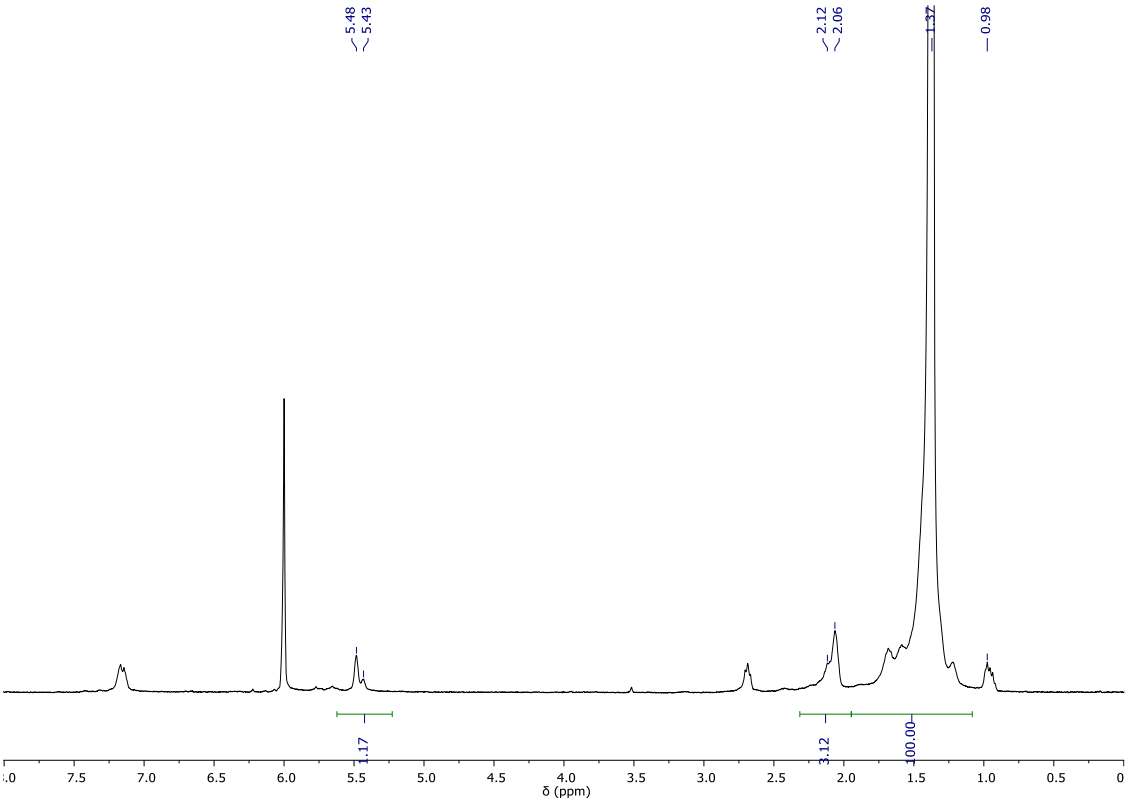

Figure S22. ^{1}H NMR (400 MHz, tetrachloroethane-*d2*) spectrum for DH-HDPE at 130 °C.

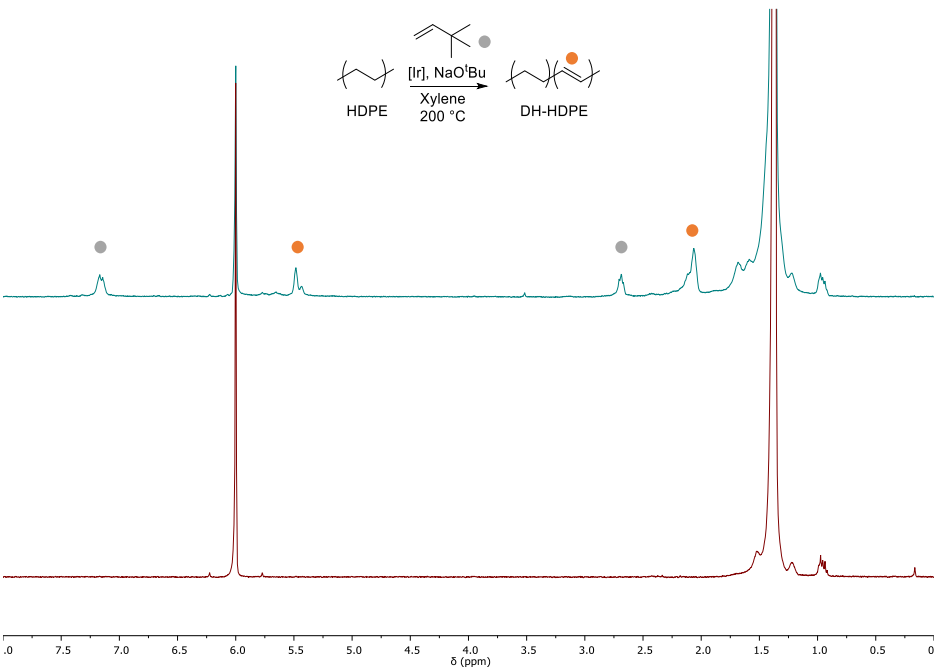

Figure S23. ^{1}H NMR (400 MHz, tetrachloroethane-*d2*) spectrum for DH-HDPE (cyan) compared with pristine HDPE (red) at 130 °C.